Carcinogenesis is a complex and long-term progress. Therefore, finding a chemopreventor and using it to inhibit the progression of PCa will be of general benefit. Our study has proved: (i) the safety of relatively long-term PCC consumption; (ii) PCC can inhibit PCa both *in vitro* and *in vivo*, and modulation of cell growth pathways may possibly be involved in suppressive effects of PCC. Other studies have reported that C3G and Pg3G, the active compounds in PCC, have antioxidant and free-radical-scavenging effects, which may protect cells from oxidative damage and reduce the risk of diabetes, cardiovascular diseases and cancer.[24–27] With further study, we can expect to determine whether the mechanism of PCC inhibition of PCa also involves these pathways. Modulation of multiple pathways can increase the chance of PCC effectively preventing PCa in humans. Taking the available information into account, PCC, a widely used food colorant, appears to be a promising chemopreventor for PCa.

Acknowledgments

This work was supported by a Grant-in-Aid for the 3rd Term Comprehensive 10-year Strategy for Cancer Control from the Ministry of Health, Labour and Welfare of Japan and a grant from the Society for Promotion of Pathology of Nagoya, Japan. The authors thank Koji Kato and Junko Takekawa for their technical assistance with immunohistochemistry.

Disclosure Statement

The authors have no conflict of interest.

References

1 Siegel R, Naishadham D, Jemal A. Cancer statistics, 2012. *CA Cancer J Clin* 2012; **62**: 10–29.
2 Huggins C, Hodges CV. The effect of castration, of estrogen and of androgen injection on serum phosphatases in metastatic carcinoma of the prostate. *Cancer Res* 1941; **1**: 293–7.
3 Rubin MA. Targeted therapy of cancer: new roles for pathologists-prostate cancer. *Mod Pathol* 2008; **21**(Suppl. 2): S44–55.
4 Wei JT, Dunn RL, Sandler HM *et al.* Comprehensive comparison of health-related quality of life after contemporary therapies for localized prostate cancer. *J Clin Oncol* 2002; **20**: 557–66.
5 Sanda MG, Dunn RL, Michalski J *et al.* Quality of life and satisfaction with outcome among prostate-cancer survivors. *N Engl J Med* 2008; **358**: 1250–61.
6 Lippman SM, Klein EA, Goodman PJ *et al.* Effect of selenium and vitamin E on risk of prostate cancer and other cancers: the selenium and vitamin E cancer prevention trial (SELECT). *JAMA* 2009; **301**: 39–51.
7 Thompson IM, Tangen CM, Goodman PJ, Lucia MS, Klein EA. Chemoprevention of prostate cancer. *J Urol* 2009; **182**(2): 499–507; discussion 508.
8 Andriole GL, Bostwick DG, Brawley OW *et al.* Effect of dutasteride on the risk of prostate cancer. *N Engl J Med* 2010; **362**: 1192–202.
9 Hagiwara A, Miyashita K, Nakanishi T *et al.* Pronounced inhibition by a natural anthocyanin, purple corn color, of 2-amino-1-methyl-6-phenylimidazo [4,5-b]pyridine (PhIP)-associated colorectal carcinogenesis in male F344 rats pretreated with 1,2-dimethylhydrazine. *Cancer Lett* 2001; **171**: 17–25.
10 Fukamachi K, Imada T, Ohshima Y, Xu J, Tsuda H. Purple corn color suppresses Ras protein level and inhibits 7,12-dimethylbenz[a]anthracene-induced mammary carcinogenesis in the rat. *Cancer Sci* 2008; **99**: 1841–6.
11 Shindo M, Kasai T, Abe A, Kondo Y. Effects of dietary administration of plant-derived anthocyanin-rich colors to spontaneously hypertensive rats. *J Nutr Sci Vitaminol (Tokyo)* 2007; **53**: 90–3.
12 Tsuda T, Horio F, Uchida K, Aoki H, Osawa T. Dietary cyanidin 3-O-beta-D-glucoside-rich purple corn color prevents obesity and ameliorates hyperglycemia in mice. *J Nutr* 2003; **133**: 2125–30.
13 Asamoto M, Hokaiwado N, Cho YM *et al.* Prostate carcinomas developing in transgenic rats with SV40 T antigen expression under probasin promoter control are strictly androgen dependent. *Cancer Res* 2001; **61**: 4693–700.
14 Cho YM, Takahashi S, Asamoto M *et al.* Age-dependent histopathological findings in the prostate of probasin/SV40 T antigen transgenic rats: lack of influence of carcinogen or testosterone treatment. *Cancer Sci* 2003; **94**: 153–7.
15 Zeng Y, Yokohira M, Saoo K *et al.* Inhibition of prostate carcinogenesis in probasin/SV40 T antigen transgenic rats by raloxifene, an antiestrogen with anti-androgen action, but not nimesulide, a selective cyclooxygenase-2 inhibitor. *Carcinogenesis* 2005; **26**: 1109–16.
16 Kandori H, Suzuki S, Asamoto M *et al.* Influence of atrazine administration and reduction of calorie intake on prostate carcinogenesis in probasin/SV40 T antigen transgenic rats. *Cancer Sci* 2005; **96**: 221–6.
17 Said MM, Hokaiwado N, Tang M *et al.* Inhibition of prostate carcinogenesis in probasin/SV40 T antigen transgenic rats by leuprorelin, a luteinizing hormone-releasing hormone agonist. *Cancer Sci* 2006; **97**: 459–67.
18 Tang M, Ogawa K, Asamoto M *et al.* Protective effects of citrus nobiletin and auraptene in transgenic rats developing adenocarcinoma of the prostate (TRAP) and human prostate carcinoma cells. *Cancer Sci* 2007; **98**: 471–7.
19 Seeni A, Takahashi S, Takeshita K *et al.* Suppression of prostate cancer growth by resveratrol in the transgenic rat for adenocarcinoma of prostate (TRAP) model. *Asian Pac J Cancer Prev* 2008; **9**: 7–14.
20 De Nunzio C, Aronson W, Freedland SJ, Giovannucci E, Parsons JK. The correlation between metabolic syndrome and prostatic diseases. *Eur Urol* 2012; **61**: 560–70.
21 Hoda MR, Mohammed N, Theil G, Fischer K, Fornara P. Obesity and prostate cancer: role of adipocytokines and clinical implications. *Urologe A* 2012; **51**: 1253–60.
22 Takeshita K, Takahashi S, Tang M, Seeni A, Asamoto M, Shirai T. Hypertension is positively associated with prostate cancer development in the TRAP transgenic rat model. *Pathol Int* 2011; **61**: 202–9.
23 Takahashi S, Takeshita K, Seeni A *et al.* Suppression of prostate cancer in a transgenic rat model via gamma-tocopherol activation of caspase signaling. *Prostate* 2009; **69**: 644–51.
24 Sun CD, Zhang B, Zhang JK *et al.* Cyanidin-3-glucoside-rich extract from Chinese bayberry fruit protects pancreatic beta cells and ameliorates hyperglycemia in streptozotocin-induced diabetic mice. *J Med Food* 2012; **15**: 288–98.
25 Delazar A, Khodaie L, Afshar J, Nahar L, Sarker SD. Isolation and free-radical-scavenging properties of cyanidin 3-O-glycosides from the fruits of Ribes biebersteinii *Berl. Acta Pharm* 2010; **60**: 1–11.
26 Xu M, Bower KA, Wang S *et al.* Cyanidin-3-glucoside inhibits ethanol-induced invasion of breast cancer cells overexpressing ErbB2. *Mol Cancer* 2010; **9**: 285.
27 Goulas V, Manganaris GA. The effect of postharvest ripening on strawberry bioactive composition and antioxidant potential. *J Sci Food Agric* 2011; **91**: 1907–14.

Supporting Information

Additional Supporting Information may be found in the online version of this article:

Fig. S1. The chemical structures of C3G, Pg3G and P3G.

Fig. S2. PCC down regulated the activity of the PSA promoter.

Fig. S3. The different stages of carcinogenesis in the prostate of TRAP rat.

Table S1. Final body and organ weights, serum hormone levels, and average PCC intake.

Cancer Science
The official journal of the Japanese Cancer Association

Apocynin, an NADPH oxidase inhibitor, suppresses rat prostate carcinogenesis

Shugo Suzuki,[1,2,5] Kazuhide Shiraga,[1] Shinya Sato,[1] Wanisa Punfa,[1,3] Aya Naiki-Ito,[1] Yoriko Yamashita,[1] Tomoyuki Shirai[1,4] and Satoru Takahashi[1]

[1]Department of Experimental Pathology and Tumor Biology, Nagoya City University Graduate School of Medical Sciences, Nagoya; [2]Pathology Division, Nagoya City East Medical Center, Nagoya, Japan; [3]Department of Biochemistry, Faculty of Medicine, Chiang Mai University, Chiang Mai, Thailand; [4]Nagoya City Rehabilitation Center, Nagoya, Japan

(Received July 12, 2013/Revised September 6, 2013/Accepted September 19, 2013/Accepted manuscript online September 30, 2013/Article first published online October 28, 2013)

Recent evidence suggests that oxidative stress contributes to the pathogenesis of prostate cancer. The present study focused on the effect of apocynin, an inhibitor of NADPH oxidase, on prostate carcinogenesis using the transgenic rat for adenocarcinoma of prostate (TRAP) model. There were no toxic effects with apocynin treatment. The percentages and numbers of carcinomas in both the ventral and lateral prostate were significantly reduced by apocynin treatment, with dose dependence. Reduction of reactive oxygen species by apocynin was confirmed by immunohistochemistry of 8-OHdG and dihydroethidium staining. Positivity of Ki67 was significantly reduced by apocynin treatment, and downregulation of clusterin expression, as well as inactivation of the MEK-ERK1/2 pathway, was a feature of the apocynin treated groups. In human prostate cancer cell line LNCaP, apocynin also inhibited reactive oxygen species production and blocked cell growth by inducing G0/G1 arrest with downregulation of clusterin and cyclin D1. These data suggest that apocynin possesses chemopreventive potential against prostate cancer. (*Cancer Sci* 2013; 104: 1711–1717)

Prostate cancer is the second most frequently diagnosed cancer in men in the world, with particularly high incidences in Oceania, Europe and North America. In Japan, incident and mortality rates for prostate cancer are relatively low are but increasing.[1,2] There are potentially curative options, such as radical prostatectomy or radiotherapy, but once the disease is metastatic, the outlook is poor. Therefore, research into chemoprevention of prostate cancer is critical.

Reactive oxygen species (ROS) can be important factors for carcinogenesis and tumor progression, not only inducing DNA damage but also producing cellular alterations, such as upregulation of MAPK and protein kinase C.[3,4] Recently, oxidative stress has been reported to contribute to cancer and progression in the prostate.[5,6] Therefore, we have focused on inhibition of ROS production as an anti-carcinogenic approach. ROS is produced by mitochondria, peroxisomes, cytochrome P-450 and other cellular elements as a byproduct, and is generated by NADPH oxidase, which is also implicated in a variety of signaling events, including cell growth, cell survival and cell death.[7] Apocynin, which belongs to the methoxy-substituted catechol family, inhibits NADPH oxidase activity by blocking the formation of NADPH oxidase complex[8] and is commonly used as a standard NOX inhibitor for research purposes.[7] In addition, apocynin can be converted by peroxidase-mediated oxidation to a dimer, which has been shown to be a more efficient inhibitor than apocynin itself.[9] We previously presented evidence that apocynin reduced oxidative stress induced by arsenite treatment of rat urothelium *in vivo*.[10]

In the present study we focus on NADPH oxidase and test whether its inhibitor, apocynin, is able to suppress prostate carcinogenesis in the transgenic rat for adenocarcinoma of prostate (TRAP) model, which was generated in our laboratory and features development of well-differentiated prostate adenocarcinomas in prostatic lobes within a short period. The TRAP rat has a transgene that encodes SV40 T antigen under probasin promoter, so that the carcinomas that develop are androgen-dependent.[11,12]

Materials and Methods

Animal experiment. Male heterozygous TRAP rats established in our laboratory with a Sprague–Dawley genetic background were used in the present study. All animals were housed in plastic cages on wood-chip bedding in an air-conditioned specific pathogen-free animal room at 22 ± 2°C and 55 ± 5% humidity with a 12 h light/dark cycle, and fed a basal diet (Oriental MF, Oriental Yeast, Tokyo, Japan) and provided water, with or without apocynin, *ad libitum*. All animal experiments were performed under protocols approved by the Institutional Animal Care and Use Committee of Nagoya City University School of Medical Sciences.

Six-week-old TRAP rats were divided into three groups of 11 rats each. The animals were given drinking water containing 0, 100 and 500 mg/L apocynin for 8 weeks and body weight and water consumption were estimated every week. At experimental week 8, under deep isoflurane anesthesia, blood was collected from 9.00 to 11.00 h to measure testosterone and estradiol hormone levels using radioimmunoassays from a commercial laboratory (SRL, Tokyo, Japan). Adiponectin concentrations in serum were determined by ELISA (adiponectin ELISA kit; Otsuka Pharmaceutical, Tokyo, Japan). The urogenital complex of each rat was removed as a whole together with the seminal vesicles, then the ventral prostate was weighed. A part of the prostate glands was immediately frozen in liquid nitrogen and stored at −80°C until processed. After that, the remaining tissue was fixed. Livers, kidneys and testes were also removed, weighed and fixed. For clusterin immunostaining, normal prostate glands from a 14-week-old male Sprague–Dawley rat were fixed. The tissues were routinely processed into paraffin-embedded sections and stained with H&E.

Histopathology and immunohistochemistry. Neoplastic lesions in the prostate gland of TRAP rats were evaluated as previously described.[13,14] Briefly, neoplastic lesions were classified into three types: low grade prostatic intraepithelial neoplasia (LG-PIN), high grade PIN (HG-PIN) and adenocarcinoma. The relative numbers of acini with the histological

[5]To whom correspondence should be addressed.
E-mail: shugo@med.nagoya-cu.ac.jp

doi: 10.1111/cas.12292

characteristics of each type, that is, LG-PIN, HG-PIN and adenocarcinoma, were quantified by counting the total acini in each prostatic lobe. Deparaffinized sections were incubated with diluted antibodies for Ki-67 (Novocastra Laboratories, Newcastle, UK), anti-8-hydroxy-2′-deoxyguanosine (8-OHdG) antibody (Japan Institute for the Control of Aging, Fukuroi, Japan), clusterin (Santa Cruz Biotechnology, Santa Cruz, CA, USA), androgen receptor (AR) and SV40 T antigen (Santa Cruz Biotechnology). The number of Ki-67-labeled or 8-OHdG-labeled cells in at least 1000 cells was counted to determine the labeling indices of HG-PIN and adenocarcinoma.

Detection of reactive oxygen species production. Six-micron frozen serial sections cut on a standard cryostat with clean blades were mounted on slides, then incubated with 5 μM dihydroethidium (Life Technologies, Carlsbad, CA, USA) in PBS for 15 min in the dark. The slides were washed two times with warm PBS and the fluorescence intensity was assessed at 518/605 nm with a spectrofluorometer. Images were also recorded with a fluorescence microscope (BZ-9000; Keyence, Osaka, Japan).

Microarray analysis. Total RNA was isolated from ventral prostate tissues en bloc by phenol–chloroform extraction (ISOGEN, Nippon Gene, Toyama, Japan). Gene expression analysis was performed using a Rat Oligo chip 20k (Toray Industries, Tokyo, Japan) according to the manufacturer's instructions. The RNA ventral prostate expression from 500 mg/L apocynin-treated rats was compared with that from control rats. After global median normalization, data cleansing was performed to remove the values for which fluorescence intensity was <100. The genes for which expression were more than twofold increased or reduced to less than half in 500 mg/L apocynin-treated rats as compared to control rats were selected.

Real-time RT-PCR. Total RNAs from ventral prostate tissues were reverse-transcribed with the ThermoScript first-strand synthesis system (Life Technologies), and real-time RT-PCR was performed using a LightCycler (Roche Diagnostics GmbH, Penzberg, Germany). The quantitative value of clusterin was normalized to endogenous cyclophilin. Clusterin RT-PCR primers were 5′-TTATGGACACAGTGGCAGAG-3′ and 5′-TACAGAACCCAGAGGAAGGA-3′. Cyclophilin RT-PCR primers were 5′-TGCTGGACCAAACACAAATG-3′ and 5′-GAAGGGGAATGAGGAAAATA-3′.

Immunoblot analyses. Ventral prostate tissues were homogenized with RIPA buffer (Pierce Biotechnology, Rockford, IL, USA) containing a protease inhibitor (Pierce Biotechnology) on ice. The insoluble matter was removed by centrifugation at 10 000*g* for 20 min at 4°C and supernatants were collected. Protein concentrations were determined with a Coomassie Plus – The Better Bradford Assay Kit (Pierce Biotechnology). Samples were mixed with 2× sample buffer (Bio-Rad Laboratories, Hercules, CA, USA) and heated for 5 min at 95°C and then subjected to SDS-PAGE. The separated proteins were transferred onto nitrocellulose membranes followed by blocking with SuperBlock Blocking Buffer (Thermo Fisher Scientific, Waltham, MA, USA) for 1 h at room temperature. Membranes were probed with antibodies for cyclin D1, clusterin, cleaved caspase-3, MEK, phospho-MEK, p44/42 MAPK (ERK1/2), phopho-ERK1/2, p38 MAPK, phospho-p38 MAPK, and caspase 3 and 7 (Cell Signaling Technology, Danvers, MA, USA) in 1× TBS with 0.1% Tween 20 at 4°C overnight, followed by exposure to peroxidase-conjugated appropriate secondary antibodies and visualization with an enhanced chemiluminescence detection system (GE Healthcare Bio-sciences, Buckinghamshire, NA, UK). To confirm equal protein loading, each membrane was stripped and reprobed with anti-β-actin (Sigma-Aldrich, St. Louis, MO, USA).

Cell line. The human androgen-dependent prostate cancer cell line LNCaP was obtained from the American Type Culture Collection (Manassas, VA, USA). The cells were grown in RPMI1640 medium with 10% FBS, 100 U/mL penicillin and 100 μg/mL streptomycin (all from Life Technologies) under an atmosphere of 95% air and 5% CO_2 at 37°C.

Cell proliferation assay. Cell proliferation of prostate cancer cell lines was assessed by 4-[3-(4-iodophenyl)-2-(4-nitrophenyl)-2H-5-tetrazolio]-1,3-benzene disulfonate tetrazolium salt (WST-1) assay (Roche Applied Science, Mannheim, Germany). Briefly, cells were seeded in 96-well plates at 500 cells/well in 200 μL of culture medium. Apocynin was added 24 h after seeding and incubated for 3 days. WST-1 reagent was added to each well with incubation for 60 min at 37°C, and then each well was measured for absorbance at 430 nm.

Detection of reactive oxygen species production in LNCaP cells. The culture supernatant was removed from all wells 24 h after apocynin treatment, and the cells were washed twice with warm PBS, then 2′,7′-dichlorofluorescin-diacetate (100 μg/mL, DCFH-DA, Sigma-Aldrich) was added with further incubation at 37°C for 20 min, in the dark. The cells were washed two times with warm RPMI1640 medium, and images were recorded using a fluorescence microscope (BZ-9000; Keyence).

Cell cycle analysis. Cells were treated with apocynin for 24 h, then suspensions were prepared and stained with propidium iodide (Guava Cell Cycle Reagent, Guava Technologies, Hayward, CA, USA) according to the Guava Cell Cycle Assay protocol. Cell cycle phase distributions were determined on a Guava PCA Instrument using CytoSoft Software.

Statistical analysis. All *in vitro* experiments were performed at least in triplicate to confirm reproducibility. Statistical analyses were performed with mean ± SD values using one-way ANOVA and Dunnett's test. Statistical significance was concluded at $*P < 0.05$, $**P < 0.01$ or $***P < 0.001$.

Results

Apocynin reduction of progression of prostate tumorigenesis as well as cell proliferation and reactive oxygen species in TRAP rats. During the experiments, water consumption by 500 mg/L apocynin-treated rats was approximately 10% lower than in the controls (Table 1). However, administration of apocynin did not cause adverse effects (e.g. impacting the growth of rats) during the study. There were no significant differences in the final body weights or in absolute and relative liver,

Table 1. Body and organ weights, water consumption

Treatment	Number of rats	Body weight (g)	Liver (g)	Kidneys (g)	Testes (g)	Ventral prostate (g)	Water consumption (mL/rat/day)
Control	11	533 ± 58	18.5 ± 2.0	3.2 ± 0.2	3.5 ± 0.4	0.30 ± 0.06	45.5 ± 4.4
100 mg/L	11	553 ± 49	20.1 ± 2.3	3.1 ± 0.3	3.6 ± 0.3	0.36 ± 0.09	46.5 ± 5.5
500 mg/L	11	558 ± 65	20.2 ± 3.2	3.2 ± 0.4	3.6 ± 0.4	0.30 ± 0.04	39.6 ± 2.6*

*Significantly different from control group, $P < 0.05$.

doi: 10.1111/cas.12292

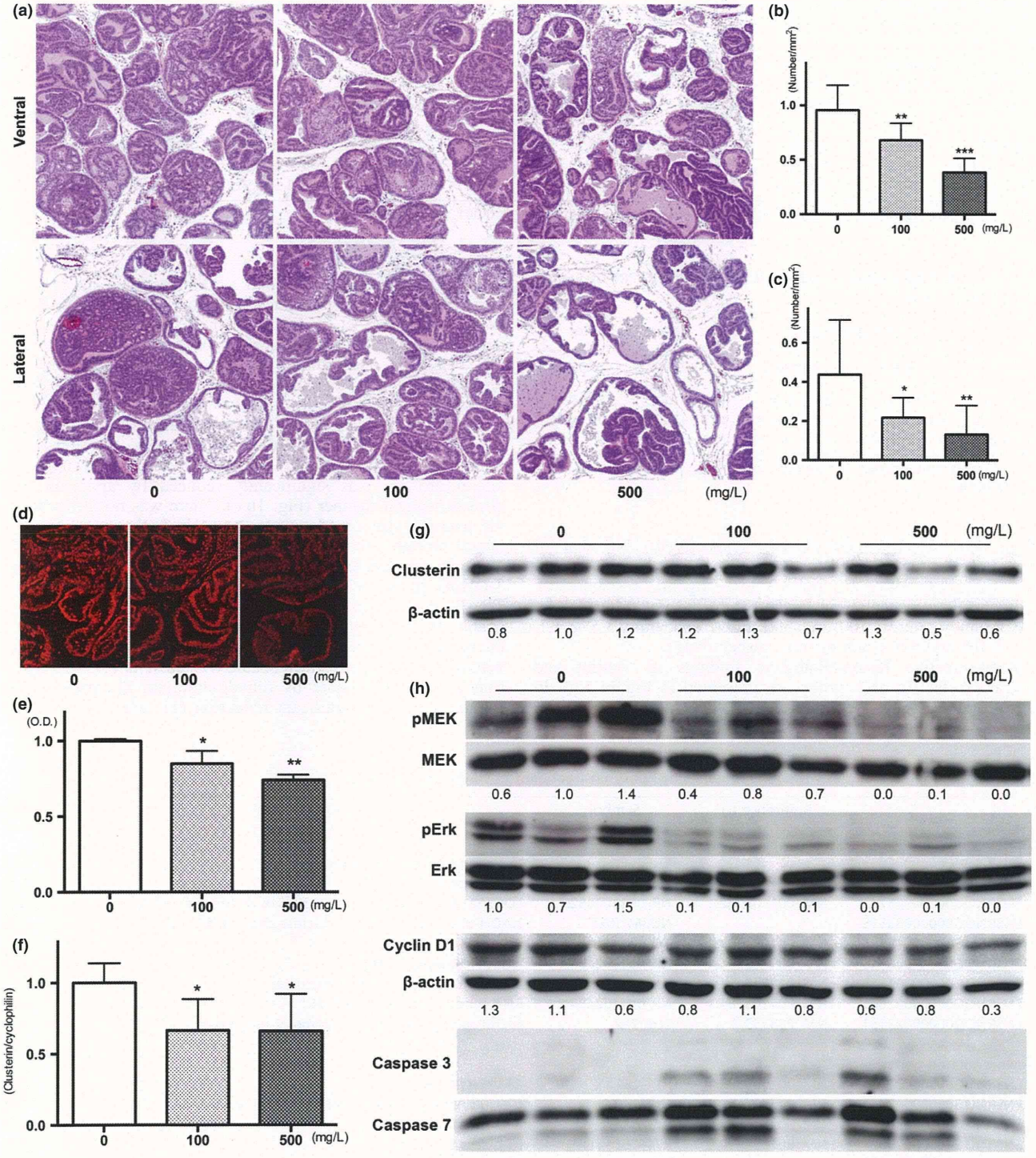

Fig. 1. Effects of apocynin on prostatic lesions. Representative histopathological findings for lesions in the ventral and lateral prostates of the controls, 100 and 500 mg/L apocynin groups (a). Number of adenocarcinoma per area in ventral (b) and lateral (c) prostate of TRAP rats treated with apocynin. Photos (d) and data (e) for reactive oxygen species production detected by dihydroethidium staining in ventral prostate of TRAP rats treated with apocynin. Expression of clusterin detected by quantitative RT-PCR (f) and western blotting (g). Results of immunoblot analysis of MAPK, cyclin D1 and caspases in ventral prostates of TRAP rats treated with apocynin. Data are mean ± SD values from 3 independent experiments. *,**,***$P < 0.05$, 0.01 and 0.001 compared to controls, respectively.

kidney, testes and prostate weights among the groups (Table 1). Histologically, there were no changes indicative of toxicity in the liver, kidneys, and testes with apocynin (data not shown). The serum level of testosterone in 500 mg/L apocynin treated rats (3.1 ± 1.6 ng/mL) was slightly higher than in other groups (control and 100 mg/L apocynin:

Table 2. Incidence of carcinoma and quantitative evaluation of neoplastic lesions in ventral and lateral prostate

Treatment	Number of rats	Ventral				Lateral			
		Incidence of carcinoma	% of lesions in prostate			Incidence of carcinoma	% of lesions in prostate		
			LG-PIN	HG-PIN	Carcinoma		LG-PIN	HG-PIN	Carcinoma
Control	11	11 (100%)	6.6 ± 2.5	81.8 ± 4.8	11.7 ± 4.5	10 (91%)	11.8 ± 5.2	82.8 ± 6.8	5.4 ± 3.9
100 mg/L	11	11 (100%)	8.0 ± 2.5	83.6 ± 3.8	8.4 ± 2.8*	10 (91%)	17.4 ± 4.3	80.1 ± 4.3	2.5 ± 1.4*
500 mg/L	11	11 (100%)	8.3 ± 1.6	87.3 ± 3.2**	4.4 ± 1.9***	6 (55%)	26.8 ± 9.9***	71.8 ± 9.0**	1.5 ± 1.7**

*,**,***Indicate significant difference from the control group, $P < 0.05$, 0.1, 0.001, respectively.

Table 3. Labeling indices of Ki67 and 8-OHdG in HG-PIN of ventral and lateral prostate

Treatment	Ventral prostate		Lateral prostate	
	Ki67	8-OHdG	Ki67	8-OHdG
Control	52.6 ± 1.1	2.9 ± 0.4	49.7 ± 1.6	2.7 ± 0.4
100 mg/L	43.8 ± 2.2***	2.3 ± 0.4**	35.2 ± 7.2***	2.0 ± 0.2***
500 mg/L	24.4 ± 1.8***	1.5 ± 0.3***	18.4 ± 2.8***	1.5 ± 0.2***

**, ***Significantly different from control group, $P < 0.01$, 0.001, respectively.

1.7 ± 1.0 and 1.9 ± 0.8 ng/mL, respectively) but that of estradiol was not affected (control, 100 and 500 mg/L apocynin: 3.2 ± 1.0, 3.4 ± 1.2 and 3.3 ± 0.7 pg/mL, respectively). Adiponection concentration in the serum did not differ among the groups (control, 100 and 500 mg/L apocynin: 3.5 ± 1.1, 3.2 ± 0.5 and 3.5 ± 0.8 ng/mL, respectively).

Representative histopathological findings of ventral and lateral prostate in each group are presented in Figure 1(a). In the ventral prostate, there was a marked or partial pathologic response to apocynin treatment, as demonstrated by a significant reduction in the prostatic neoplastic lesions in TRAP rats; however, small foci of PIN remained. Decrease in the incidence of adenocarcinoma was also observed in the lateral prostate (Table 2). Quantitative evaluation of the proportion of preneoplastic and neoplastic lesions in the prostate gland showed significant suppression of progression from LG-PIN or HG-PIN to adenocarcinoma in rats treated with apocynin in a dose-dependent manner (Table 2). To focus on adenocarcinoma, the number of foci per area in both the ventral and lateral prostate was significantly reduced by apocynin in a dose-dependent manner (Fig. 1b,c). There was no difference in the average size of adenocarcinomas in both the ventral and lateral prostate among the groups (data not shown). There was a significant decrease in the labeling index of Ki-67 and 8-OHdG in HG-PIN of the ventral and lateral prostates of TRAP rats given apocynin in a dose-dependent manner (Table 3). Although the rate of significance was slightly less, the results were mostly the same in the adenocarcinoma of the ventral and lateral prostates (Table S1). Results for ROS detection in ventral prostate by dihydroethidium are presented in Figure 1(d), with significant reduction (11 and 22% reduction

Table 4. Upregulated and downregulated genes by apocynin treatment in ventral prostate

ID	Reference ID	Symbol	Description	Ratio
Upregulated genes				
ENSRNOG00000038093	–	LAC2_RAT	Ig lambda-2 chain C region	5.62
ENSRNOG00000033745	–	Q5FVP9_RAT	Cfh protein	3.10
ENSRNOG00000005743	NM_001108582.1	NP_001102052.1	LOC362136 (predicted) (RGD1309610_predicted), mRNA	2.58
ENSRNOG00000033615	–	NU3M_RAT	NADH-ubiquinone oxidoreductase chain 3 (EC 1.6.5.3)	2.45
ENSRNOG00000015155	NM_001037351.1	Tnnc2	Troponin C2, fast	2.11
ENSRNOG00000008746	NM_001108594.1	NP_001102064.1	Histidyl tRNA synthetase 2	2.07
ENSRNOG00000001333	NM_012826.1	Azgp1	Zinc-alpha-2-glycoprotein precursor	2.06
ENSRNOG00000002871	NM_001108984.1	NP_001102454.1	RNA binding motif protein 25	2.05
ENSRNOG00000023151	NM_203333.2	Scgb2a2	Secretoglobin family 2A member 2 precursor	2.01
Downregulated genes				
ENSRNOG00000021604	NM_001008835.1	RT1-CE1	RT1 class I, CE1	0.28
ENSRNOG00000002343	NM_017237.2	Uchl1	Ubiquitin carboxyl-terminal hydrolase isozyme L1 (EC 3.4.19.12)	0.36
ENSRNOG00000038999	NM_001008827.1	RT1-A1	RT1 class Ia, locus A1	0.36
ENSRNOG00000029579	NM_001008840.1	RT1-CE2	RT1 class I, CE2	0.41
ENSRNOG00000030251	–	RT1-CE10	RT1 class I, CE10	0.41
ENSRNOG00000032872	–	UBIQ_RAT	Ubiquitin	0.43
ENSRNOG00000034234	–	COX1_RAT	Cytochrome c oxidase subunit 1 (EC 1.9.3.1)	0.43
ENSRNOG00000037414	–	Q5I1B4_RAT	ABP beta (Fragment)	0.44
ENSRNOG00000030371	–	COX2_RAT	Cytochrome c oxidase subunit 2	0.45
ENSRNOG00000039668	NM_001107100.1	NP_001100570.1	Procollagen, type VIII, alpha 1	0.46
ENSRNOG00000016460	NM_053021.2	Clu	Clusterin precursor	0.49
ENSRNOG00000011647	NM_053485.2	S100a6	Protein S100-A6	0.50
ENSRNOG00000007539	NM_138881.1	Best5	Radical S-adenosyl methionine domain-containing protein 2	0.50
ENSRNOG00000002052	NM_022543.2	Ssg1	Coiled-coil domain-containing protein 80 precursor	0.50

doi: 10.1111/cas.12292

at 100 and 500 mg/L, respectively) documented (Fig. 1e). Androgen receptors and SV40 T antigen were diffusely detected immunohistochemically in areas of PIN and adenocarcinomas in the ventral and lateral prostate, with no differences among the groups (data not shown).

Reduction of cell proliferation by apocynin treatment was associated with changes in clusterin and the MEK-ERK1/2 pathway. To elucidate the mechanisms of anti-carcinogenesis of apocynin, microarray analysis was performed (GEO: GSE47200). Genes that were upregulated or downregulated by apocynin are listed in Table 4. After selection, 9 upregulated and 14 downregulated genes were detected, some related to oxidative responses (NADH-ubiquinone oxidoreductase chain 3, cytochrome c oxidase subunit 1 and 2) and others immunological responses (Ig lambda-2 chain C region, Cfh protein, secretoglobin family 2A member 2 precursor, RT1 class I, CE1, CE2 and CE10, RT1 class Ia, locus A1). Because apocynin reduced rat prostate carcinogenesis, we focused on the clusterin precursor belonging to downregulated genes, which is known to be related to tumorigenesis in many sites. Reduction of clusterin expression in the ventral prostate of apocynin-treated rats was confirmed by real-time RT-PCR (Fig. 1f) and also by western blotting (Fig. 1g). Immunohistochemical analyses revealed that clusterin expression was observed mainly in the epithelial membranes of the ventral prostate of TRAP rats, but no staining was observed in the epithelium of the prostate of Sprague–Dawley rats (Fig. S1a). Differences in the intensity of clusterin immunostaining determined by optical density measurement was relatively inconspicuous among LG-PIN, HG-PIN or adenocarcinoma in the ventral lobes of the control TRAP rats (Fig. S1b). However, clusterin expression in HG-PIN of ventral prostate of apocynin-treated TRAP rats was significantly reduced compared to the control (Fig. S1c; control, 100 and 500 mg/L apocynin: 50.1 ± 5.0, 43.2 ± 7.4 and 35.6 ± 4.3, respectively). Reduction of phosphorylation in MEK and p44/42 MAPK (ERK1/2), and cyclin D1 were also detected. Cleaved caspases 3 and 7 were detected in the ventral prostate of some apocynin-treated rats (Fig. 1h).

Apocynin affected reduction of cell growth via the same pathways in a human prostate cancer cell line. In the human prostate cell line, significant reduction of cell growth and ROS generation was detected after apocynin treatment at concentrations higher than 250 μM (Fig. 2a,b). Apocynin-treated cells appeared to accumulate in G1 phase at 500 μM, compared to the controls ($P < 0.05$), with concomitant decrease in the percentage of cells in the S phase (Fig. 2c). Downregulation of clusterin around 70 kDa and cyclin D1 expression were detected by western blotting (Fig. 2d).

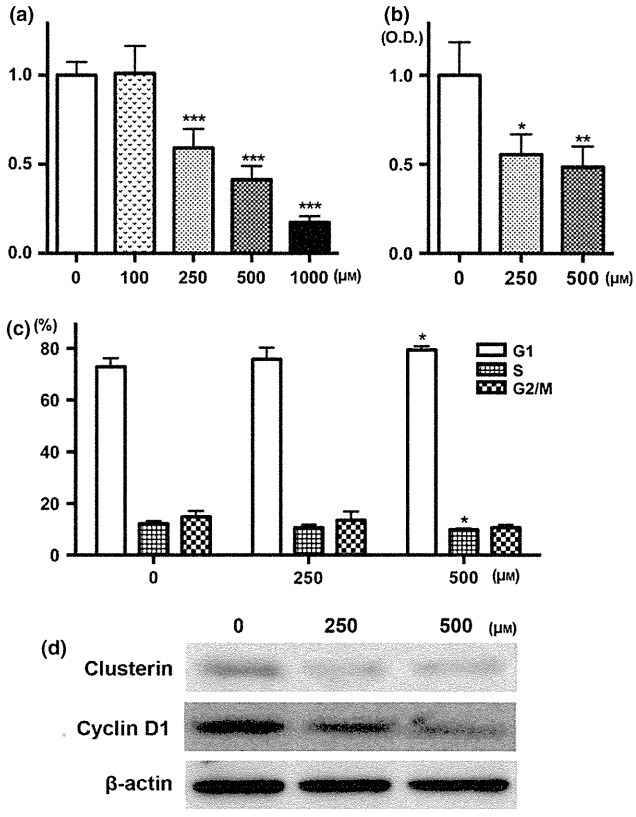

Fig. 2. Anti-growth effects of apocynin in LNCaP cells. Cells were incubated with apocynin for 72 h and then cytotoxicity was assessed by WST-1 assay (a). Reactive oxygen species production data detected by DCFH-DA after apocynin treatment for 24 h (b). Cell cycle distribution of LNCaP cells after treatment with apocynin for 24 h (c). Immunoblot analysis of the protein levels of clusterin, cyclin D1 and ß-actin with apocynin treatment (d). $*P < 0.05$, $**P < 0.01$ and $***P < 0.001$ compared to controls. O.D, optical density.

Discussion

In the present study, we demonstrated suppressive effects of apocynin treatment on prostatic carcinogenesis in the TRAP rat model. Because apocynin is known to be an NADPH oxidase inhibitor, we focused on ROS conditions in prostate tissue using immunohistochemistry for 8-OHdG and dihydroethidium staining. Some reports have indicated that antioxidants such as N-acetylcysteine and vitamin C clearly reduce oxidative stress *in vitro*, but exert less effects with oral dosing *in vivo*.[15,16] ROS is generally produced from mitochondria, peroxisomes, cytochrome P450 and NADPH oxidase.[4,6,7] Apocynin only affects ROS reduction from NADPH oxidase, but it would be expected to be a good antioxidant *in vivo*. In addition, we did not detect any toxic effects of apocynin in this study.

Reactive oxygen species generation is not only considered associated with tissue injury and/or DNA damage, but also neoplastic transformation, aberrant growth and/or proliferation.[4,7] Indeed, ROS may play broad roles in cellular processes associated with initiation and development of many cancers, including prostate cancer.[6] In this study, apocynin reduced the Ki-67 labeling index and cyclin D1 expression, which indicates that ROS generation is related to cell proliferation in prostate lobes of TRAP rats. Furthermore, NADPH oxidase is reported to regulate plasma adiponectin,[17] whose concentration may be negatively correlated with prostate cancer progression.[18] Therefore, we investigated adiponectin concentration in serum, but did not find any differences among the groups.

In TRAP rats, we previously detected activation of p38 MAPK and ERK1/2 in prostate tissue, and inactivation by chemopreventive agents such as angiotensin II receptor blocker or purple corn color.[14,19] These also reduced cell proliferation and/or induced apoptosis in prostate tissue. In this study, we also detected dephosphorylation of ERK1/2 in the prostate after apocynin treatment. To assess the relationship between ROS generation and phosphorylation of ERK1/2, microarray analysis was employed. The data obtained for upregulated and downregulated genes indicated associations with ROS generation, immune function and translation by gene ontology.[20] We focused on clusterin, dysregulated in many types of cancer, including prostate cancer,[21] with cellular functions such as a sulfated glycoprotein in regulation of apoptosis, cell cycle control, DNA repair, cell adhesion and tissue remodeling.[22,23] It has two isoforms. Secretory clusterin (sCLU) has a chaperone

action like that of small heat shock proteins, and is sized around 70–80 kDa. The other clusterin isoform is the nuclear form (nCLU) of 55 kDa, associated with cell death.[21–23] In this study, we detected significant reduction of clusterin protein around 70 kDa. Because sCLU is reported to be downregulated by p53 in some tumor cells,[22] high expression of clusterin in the prostate would be expected given dysfunction of p53 under the influence of SV40 T antigen in TRAP rats.[24]

In human prostate cancer, clusterin expression is initially low in contrast with the prostate cancer cells resistant to conventional chemotherapy or hormonal therapy which show upregulation.[21,25] Meanwhile, we detected rather high expression of clusterin in all stages of prostate cancer development in TRAP rats. In te transgenic adenocarcinoma of mouse prostate (TRAMP) model, higher expression of clusterin in the prostate glands was detected compared to that in non-transgenic mice; however, analyses of overt carcinoma revealed no expression.[26] These data suggest that SV40 T antigen supports to induce clusterin expression among the carcinogenic process in the prostate of both mice and rats. The difference in clusterin expression in carcinoma may be related to the different histology between mice (poorly-differentiated neuroendocrine-like carcinomas) and rats (moderately differentiated adenocarcinomas), because clusterin is mainly stained in the membrane.

Recently, sCLU was reported to induce phosphorylation of ERK1/2 in lung adenocarcinoma and pancreatic cancer cells.[27,28] Therefore, we considered that apocynin reduced prostate carcinogenesis via clusterin, acting on the ERK1/2 pathway and reducing cell proliferation in TRAP rats. We also found that apocynin reduced cell growth and ROS generation, along with expression of clusterin and cyclin D1 in LNCaP cells (human prostate cell line). Although there is a possibility that the exact intracellular molecular pathways affected by apocynin treatment may be different between humans and rats, we suggest that there may be similar anti-neoplastic effects caused by apocynin, especially related to clusterin expression, in rat and human prostate.

Chemoprevention attempts are comprehensive in prostate cancer, and various agents are reported to prevent, reverse or delay tumor deveolpment and progression.[29] In this study, we detected lower incidence of adenocarcinoma in the lateral lobes of 500 mg/L apocynin-treated rats, and reduction of cell proliferation was observed in both PIN and adenocarcinoma. Thus, we consider that apocynin has potential to prevent and delay the carcinogenic process, and is suitable as a chemopreventive drug. Recently, custirsen (OGX-011), a clusterin inhibitor, was selected for use as an anti-cancer drug in a randomized phase II study of patients with metastatic castration-resistant prostate cancer.[30,31] We earlier reported that apocynin inhibited growth of androgen-independent prostate cancer with inhibition of phosphorylation of Rac1 and NF-κB and angiogenesis.[32] Together with the present data, we confirm that apocynin has the potential to be a candidate anti-cancer drug for androgen-dependent/independent prostate cancer.

In conclusion, apocynin, an NADPH oxidase inhibitor, suppressed prostate carcinogenesis while reducing ROS in the TRAP rat model. The mechanism of prevention appears to involve regulation of cell proliferation via clusterin and the MEK-ERK1/2 pathway. Apocynin warrants further attention as a promising chemopreventive drug for prostate cancer.

Acknowledgments

This work was supported by a Grant-in-Aid for the 3rd Term Comprehensive 10-Year Strategy for Cancer Control from the Ministry of Health, Labour and Welfare of Japan and grants from Ono Pharmaceutical, the Society for Promotion of Pathology in Nagoya, and the Research Foundation for Oriental Medicine. The authors would like to thank Dr Malcolm Moore for his help in reviewing this manuscript.

Disclosure Statement

The authors have no conflict of interest.

References

1 Jemal A, Bray F, Center MM, Ferlay J, Ward E, Forman D. Global cancer statistics. *CA Cancer J Clin* 2011; **61**: 69–90.
2 Damber JE, Aus G. Prostate cancer. *Lancet* 2008; **371**: 1710–21.
3 Lee YJ, Lee JH, Han HJ. Extracellular adenosine triphosphate protects oxidative stress-induced increase of p21(WAF1/Cip1) and p27(Kip1) expression in primary cultured renal proximal tubule cells: role of PI3K and Akt signaling. *J Cell Physiol* 2006; **209**: 802–10.
4 Wu WS. The signaling mechanism of ROS in tumor progression. *Cancer Metastasis Rev* 2006; **25**: 695–705.
5 Kumar B, Koul S, Khandrika L, Meacham RB, Koul HK. Oxidative stress is inherent in prostate cancer cells and is required for aggressive phenotype. *Cancer Res* 2008; **68**: 1777–85.
6 Khandrika L, Kumar B, Koul S, Maroni P, Koul HK. Oxidative stress in prostate cancer. *Cancer Lett* 2009; **282**: 125–36.
7 Bedard K, Krause KH. The NOX family of ROS-generating NADPH oxidases: physiology and pathophysiology. *Physiol Rev* 2007; **87**: 245–313.
8 Stolk J, Hiltermann TJ, Dijkman JH, Verhoeven AJ. Characteristics of the inhibition of NADPH oxidase activation in neutrophils by apocynin, a methoxy-substituted catechol. *Am J Respir Cell Mol Biol* 1994; **11**: 95–102.
9 Stefanska J, Pawliczak R. Apocynin: molecular aptitudes. *Mediators Inflamm* 2008; **2008**: 106507.
10 Suzuki S, Arnold LL, Pennington KL, Kakiuchi-Kiyota S, Cohen SM. Effects of co-administration of dietary sodium arsenite and an NADPH oxidase inhibitor on the rat bladder epithelium. *Toxicology* 2009; **261**: 41–6.
11 Asamoto M, Hokaiwado N, Cho YM *et al.* Prostate carcinomas developing in transgenic rats with SV40 T antigen expression under probasin promoter control are strictly androgen dependent. *Cancer Res* 2001; **61**: 4693–700.
12 Cho YM, Takahashi S, Asamoto M *et al.* Age-dependent histopathological findings in the prostate of probasin/SV40 T antigen transgenic rats: lack of influence of carcinogen or testosterone treatment. *Cancer Sci* 2003; **94**: 153–7.
13 Seeni A, Takahashi S, Takeshita K *et al.* Suppression of prostate cancer growth by resveratrol in the transgenic rat for adenocarcinoma of prostate (TRAP) model. *Asian Pac J Cancer Prev* 2008; **9**: 7–14.
14 Long N, Suzuki S, Sato S *et al.* Purple corn color inhibition of prostate carcinogenesis by targeting cell growth pathways. *Cancer Sci* 2013; **104**: 298–303.
15 Wang Z, Zhou J, Lu X, Gong Z, Le XC. Arsenic speciation in urine from acute promyelocytic leukemia patients undergoing arsenic trioxide treatment. *Chem Res Toxicol* 2004; **17**: 95–103.
16 Gibson KR, Neilson IL, Barrett F *et al.* Evaluation of the antioxidant properties of N-acetylcysteine in human platelets: prerequisite for bioconversion to glutathione for antioxidant and antiplatelet activity. *J Cardiovasc Pharmacol* 2009; **54**: 319–26.
17 Furukawa S, Fujita T, Shimabukuro M *et al.* Increased oxidative stress in obesity and its impact on metabolic syndrome. *J Clin Invest* 2004; **114**: 1752–61.
18 Goktas S, Yilmaz MI, Caglar K, Sonmez A, Kilic S, Bedir S. Prostate cancer and adiponectin. *Urology* 2005; **65**: 1168–72.
19 Takahashi S, Uemura H, Seeni A *et al.* Therapeutic targeting of angiotensin II receptor type 1 to regulate androgen receptor in prostate cancer. *Prostate* 2012; **72**: 1559–72.
20 Ashburner M, Ball CA, Blake JA *et al.* Gene ontology: tool for the unification of biology. The Gene Ontology Consortium. *Nat Genet* 2000; **25**: 25–9.
21 Rizzi F, Bettuzzi S. The clusterin paradigm in prostate and breast carcinogenesis. *Endocr Relat Cancer* 2010; **17**: R1–17.
22 Shannan B, Seifert M, Leskov K *et al.* Challenge and promise: roles for clusterin in pathogenesis, progression and therapy of cancer. *Cell Death Differ* 2006; **13**: 12–9.
23 Shannan B, Seifert M, Boothman DA, Tilgen W, Reichrath J. Clusterin and DNA repair: a new function in cancer for a key player in apoptosis and cell cycle control. *J Mol Histol* 2006; **37**: 183–8.

doi: 10.1111/cas.12292

24 Ahuja D, Saenz-Robles MT, Pipas JM. SV40 large T antigen targets multiple cellular pathways to elicit cellular transformation. *Oncogene* 2005; **24**: 7729–45.
25 Rizzi F, Bettuzzi S. Clusterin (CLU) and prostate cancer. *Adv Cancer Res* 2009; **105**: 1–19.
26 Caporali A, Davalli P, Astancolle S *et al.* The chemopreventive action of catechins in the TRAMP mouse model of prostate carcinogenesis is accompanied by clusterin over-expression. *Carcinogenesis* 2004; **25**: 2217–24.
27 Chou TY, Chen WC, Lee AC, Hung SM, Shih NY, Chen MY. Clusterin silencing in human lung adenocarcinoma cells induces a mesenchymal-to-epithelial transition through modulating the ERK/Slug pathway. *Cell Signal* 2009; **21**: 704–11.
28 Tang Y, Liu F, Zheng C, Sun S, Jiang Y. Knockdown of clusterin sensitizes pancreatic cancer cells to gemcitabine chemotherapy by ERK1/2 inactivation. *J Exp Clin Cancer Res* 2012; **31**: 73.
29 Gupta S. Prostate cancer chemoprevention: current status and future prospects. *Toxicol Appl Pharmacol* 2007; **224**: 369–76.
30 Saad F, Hotte S, North S *et al.* Randomized phase II trial of Custirsen (OGX-011) in combination with docetaxel or mitoxantrone as second-line therapy in patients with metastatic castrate-resistant prostate cancer progressing after first-line docetaxel: CUOG trial P-06c. *Clin Cancer Res* 2011; **17**: 5765–73.
31 Chi KN, Hotte SJ, Yu EY *et al.* Randomized phase II study of docetaxel and prednisone with or without OGX-011 in patients with metastatic castration-resistant prostate cancer. *J Clin Oncol* 2010; **28**: 4247–54.
32 Suzuki S, Pitchakarn P, Sato S, Shirai T, Takahashi S. Apocynin, an NADPH oxidase inhibitor, suppresses progression of prostate cancer via Rac1 dephosphorylation. *Exp Toxicol Pathol* 2013; **65**: 1035–41.

Supporting Information

Additional supporting information may be found in the online version of this article:

Fig. S1. Expression of clusterin in ventral lobe of prostate. Pictures of H&E and immunohistochemistry of clusterin in normal epithelium in Sprague–Dawley rat, LG-PIN, HG-PIN and carcinoma in TRAP rats (a) and expression of clusterin (b). Expression of clusterin in HG-PIN of ventral lobe of control, 100 and 500 mg/L apocynin treated rats (c). Carcinoma; Adenocarcinoma. *,***$P < 0.05$ and 0.001 compared to Normal epithelium or control, respectively.

Table S1. Labeling indices of Ki67 and 8-OHdG in adenocarcinoma of ventral and lateral prostate.

Oncogene (2013) **32,** 2140–2149

www.nature.com/onc

ORIGINAL ARTICLE

FHL1 on chromosome X is a single-hit gastrointestinal tumor-suppressor gene and contributes to the formation of an epigenetic field defect

K Asada[1,7], T Ando[1,2,7], T Niwa[1], S Nanjo[1], N Watanabe[1], E Okochi-Takada[1], T Yoshida[1], K Miyamoto[3], S Enomoto[4], M Ichinose[4], T Tsukamoto[5], S Ito[6], M Tatematsu[5], T Sugiyama[2] and T Ushijima[1]

Tumor-suppressor genes on chromosome X can be inactivated by a single hit, any of the point mutations, chromosomal loss and aberrant DNA methylation. As aberrant DNA methylation can be induced frequently, we here aimed to identify a tumor-suppressor gene on chromosome X inactivated by promoter DNA methylation. Of 69 genes on chromosome X upregulated by treatment of a gastric cancer cell line with a DNA-demethylating agent, 5-aza-2′-deoxycytidine, 11 genes had low or no expression in the cell line and abundant expression in normal gastric mucosae. Among them, *FHL1* was frequently methylation-silenced in gastric and colon cancer cell lines, and methylated in primary gastric (21/80) and colon (5/50) cancers. Knockdown of the endogenous *FHL1* in two cell lines by two kinds of shRNAs significantly increased cell growth *in vitro* and sizes of xenografts in nude mice. Expression of exogenous *FHL1* in a non-expressing cell line significantly reduced its migration, invasion and growth. Notably, a somatic mutation (G642T; Lys214Asn) was identified in one of 144 colon cancer specimens, and the mutant *FHL1* was shown to lack its inhibitory effects on migration, invasion and growth. *FHL1* methylation was associated with *Helicobacter pylori* infection and accumulated in normal-appearing gastric mucosae of gastric cancer patients. These data showed that *FHL1* is a methylation-silenced tumor-suppressor gene on chromosome X in gastrointestinal cancers, and that its silencing contributes to the formation of an epigenetic field for cancerization.

Oncogene (2013) **32,** 2140–2149; doi:10.1038/onc.2012.228; published online 11 June 2012

Keywords: field for cancerization; chromosome X; DNA methylation; gastrointestinal cancer; *Helicobacter pylori*

INTRODUCTION

Inactivation of tumor-suppressor genes is deeply involved in cancer development and progression.[1] The vast majority of tumor-suppressor genes are somatically inactivated by two hits of both alleles by genetic and/or epigenetic mechanisms, such as point mutations, chromosomal deletions and aberrant DNA methylation of promoter CpG islands (CGIs).[2,3] The two-hit theory makes tumor-suppressor genes on chromosome X unique because they can be inactivated by a single hit, and thus are 'risky' genes. So far, three examples have been identified, including *WTX* in Wilms tumors,[4] *FOXP3* in breast and prostate cancers[5,6] and *PHF6* in T-cell acute lymphoblastic leukemia (T-ALL),[7] all of which are inactivated by a point mutation or chromosomal loss.

Among the mechanisms of tumor-suppressor gene inactivation, aberrant DNA methylation can be present not only in tumor tissues but also in normal-appearing tissues, such as non-cancerous tissues of gastric,[8,9] colon,[10] liver,[11] esophageal,[12–14] breast[15] and renal cancer patients.[16] Levels of aberrant DNA methylation in non-cancerous tissues correlate with cancer risk clearly for gastric cancers[8,17] and other cancers, and accumulation of aberrant DNA methylation in a tissue is considered to form an epigenetic field for cancerization (epigenetic field defect).[18] Such association has been analyzed using methylation levels of marker genes, which are methylated in association with various tumor-suppressor genes and show much higher levels, and only a limited number of genes that functionally contribute to the field defect have been identified.

To identify risky genes that contribute to the formation of an epigenetic field defect, we here searched for genes on chromosome X from the 495 genes whose expression was upregulated fourfold or more after treatment with a DNA-demethylating agent, 5-aza-2′-deoxycytidine (5-aza-dC)[19] of a gastric cancer cell line (AGS), which is known to have very frequent methylation of CGIs.[20]

RESULTS

Screening of methylation-silenced genes on chromosome X

Among the 495 genes whose expression was upregulated fourfold or more by treatment of the AGS gastric cancer cell line with 5-aza-dC, 69 genes were located on chromosome X. Among the 69 genes, 11 genes had low expression (signal intensity <200) in non-treated AGS cells and had high expression (signal intensity >500) in a pool of gastric mucosae of three healthy volunteers.

[1]Division of Epigenomics, National Cancer Center Research Institute, Tokyo, Japan; [2]Third Department of Internal Medicine, University of Toyama, Toyama, Japan; [3]Institute for Clinical Research and Department of Surgery, National Hospital Organization Kure Medical Center/Chugoku Cancer Center, Hiroshima, Japan; [4]Second Department of Internal Medicine, Wakayama Medical University, Wakayama, Japan; [5]Division of Oncological Pathology, Aichi Cancer Center Research Institute, Nagoya, Japan and [6]Department of Gastroenterological Surgery, Aichi Cancer Center Hospital, Nagoya, Japan. Correspondence: Dr T Ushijima, Division of Epigenomics, National Cancer Center Research Institute, 5-1-1 Tsukiji, Chuo-ku, Tokyo 104-0045, Japan.
E-mail: tushijim@ncc.go.jp
[7]These authors contributed equally to this work.
Received 20 September 2011; revised 25 April 2012; accepted 4 May 2012; published online 11 June 2012

Genomic structures were analyzed for these 11 genes, and eight of them had CGIs in their promoter regions (Supplementary Table 1). Their mRNA expression levels were confirmed by quantitative reverse transcription–PCR (qRT–PCR) in non-treated AGS cells and gastric epithelial cells obtained by the gland isolation technique, and five (*MAOA, CXorf26, FHL1, SMARCA1* and *MAOB*) had consistent expression in gastric epithelial cells (Supplementary Table 1). Among the five genes, we focused on the *FHL1* gene, because it was reported to be able to inhibit growth, migration, invasion and metastasis of multiple types of cancer cells.[21–26] The other four genes were not reported to be involved in cancer development in the literature.

Promoter methylation and silencing of *FHL1* in gastrointestinal cancer cell lines

DNA methylation status of the *FHL1* promoter region was analyzed using two sets of methylation-specific PCR (MSP) primers designed to cover a region from the transcription start site to 220 bp upstream (Figure 1a). Among the 73 cancer cell lines analyzed (11 gastric, 7 colon, 12 lung, 12 skin, 7 pancreas, 4 esophageal, 4 prostate, 6 breast and 10 ovary cancer cell lines; Supplementary Table 2), *FHL1* was completely methylated (no unmethylated DNA molecules detected) in seven gastric, three colon (Figure 1b) and one lung cancer cell lines. In normal-appearing gastric and colonic mucosae, and peripheral leukocytes of healthy volunteers, *FHL1* was completely unmethylated in males, and partially methylated in females (Figure 1c). The partial methylation in females was considered to reflect methylation of the inactive chromosome X, which is shown later.

The role of the promoter methylation in downregulation of *FHL1* expression was analyzed. First, an association between the methylation and loss of expression was confirmed among the 11 gastric and 7 colon cancer cell lines. *FHL1* was consistently unexpressed in seven gastric and three colon cancer cell lines with its complete methylation (Figures 2a and b), but was expressed in most of the cancer cell lines without methylation, in normal colonic epithelial cells (CRL1790 and CRL1831) and in normal-appearing gastric and colonic mucosae. Second, when promoter methylation was removed by 5-aza-dC treatment of AGS and

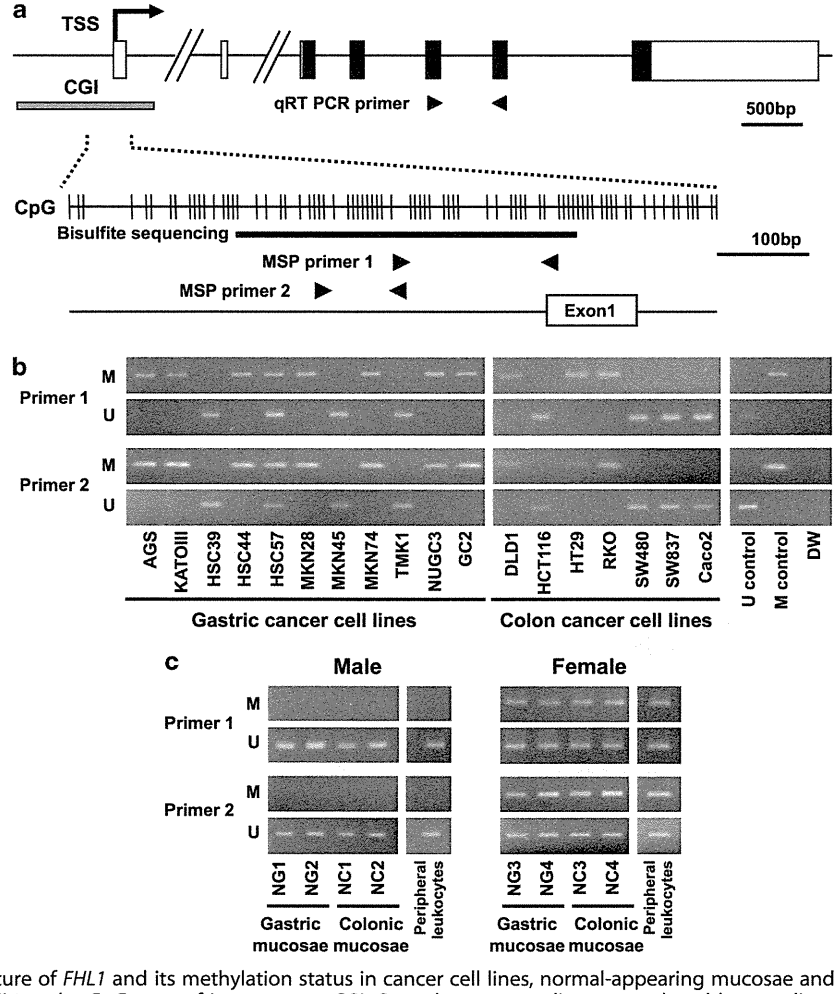

Figure 1. Genomic structure of *FHL1* and its methylation status in cancer cell lines, normal-appearing mucosae and peripheral leukocytes. (**a**) Genomic structure of *FHL1* and a CpG map of its promoter CGI. Open box, non-coding exon; closed box, coding exon; arrow, transcription start site (TSS); gray box, CGI region; vertical lines, individual CpG sites; arrowheads, primers for qRT–PCR and MSP; and bold line and number, the region and individual CpG sites analyzed by bisulfite sequencing. (**b**) Promoter methylation of *FHL1* in 11 gastric and seven colon cancer cell lines analyzed by MSP. M and U, primer sets specific to methylated and unmethylated DNA, respectively; U control, fully unmethylated genomic DNA; and M control, fully methylated genomic DNA. *FHL1* was frequently methylated in gastric and colon cancer cell lines. (**c**) Promoter methylation of *FHL1* in male and female normal-appearing gastric and colonic mucosae and peripheral leukocytes. *FHL1* was completely unmethylated in males and partially methylated in females.

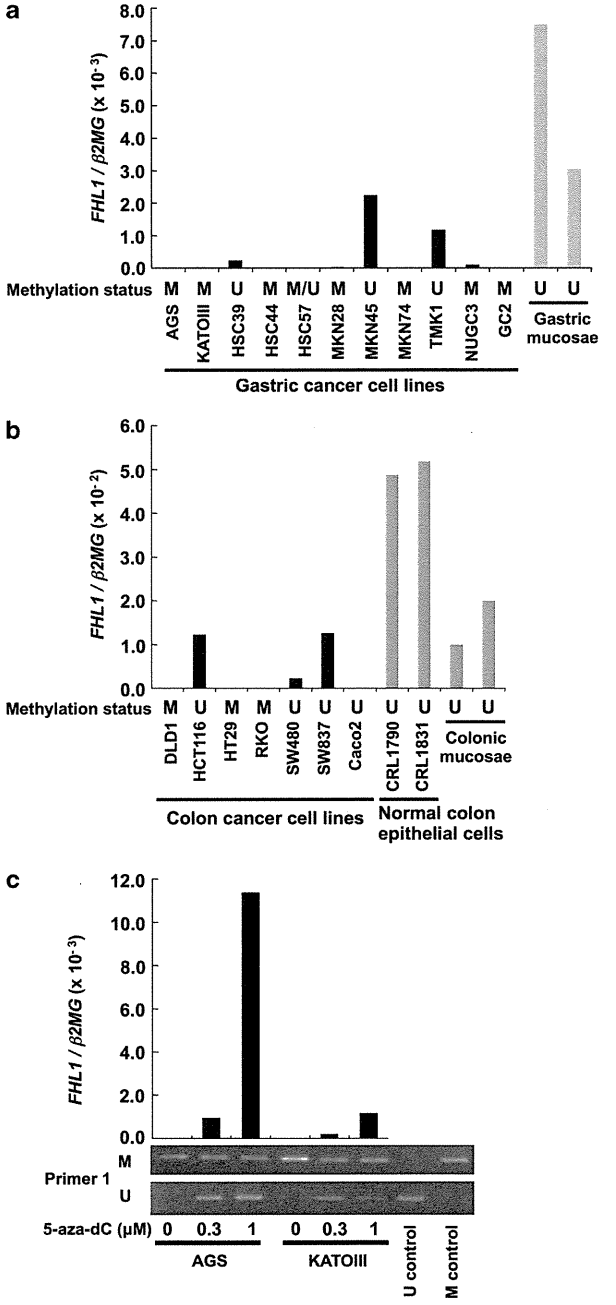

Figure 2. Methylation-silencing of *FHL1* in gastrointestinal cancer cell lines. (**a**) qRT–PCR of *FHL1* in gastric cancer cell lines and normal-appearing gastric mucosae. Results of MSP in Figure 1b are shown by M, M/U and U. M, only methylated DNA detected; M/U, both methylated and unmethylated DNA detected; and U, only unmethylated DNA detected. *FHL1* was not expressed in cell lines with complete methylation. (**b**) qRT–PCR of *FHL1* in colon cancer cell lines, normal colonic epithelial cells and normal-appearing colonic mucosae. *FHL1* was not expressed in cell lines with complete methylation. (**c**) Re-expression and demethylation of *FHL1* after 5-aza-dC treatment of AGS and KATOIII. *FHL1* expression was induced, along with its demethylation, after treatment with 5-aza-dC. U control, fully unmethylated genomic DNA; and M control, fully methylated genomic DNA.

KATOIII gastric cancer cell lines, *FHL1* expression was restored (Figure 2c). These data demonstrated that promoter methylation of *FHL1* caused its silencing.

Methylation of *FHL1* in surgical gastrointestinal cancer specimens

FHL1 methylation in surgical cancer specimens was analyzed by quantitative real-time MSP (qMSP) of 80 gastric and 50 colon cancers derived from male patients (Figure 3a). We adopted a cutoff value of 6%, which was previously determined based on the lowest methylation levels of tumor-suppressor genes in cancer samples,[9,27] and was also used in other researchers' report.[28] *FHL1* was methylated in 21 of the 80 (26%) gastric cancers and 5 of the 50 (10%) colon cancers. The presence of dense methylation of the promoter region was confirmed by bisulfite sequencing, and the fraction of densely methylated DNA molecules was in accordance with the methylation level obtained by qMSP (Figure 3b).

Association between promoter methylation and decreased expression was analyzed in 33 cancer specimens for which RNA was available. The mean *FHL1* expression level of 11 cancers with methylation was significantly lower than that of 22 cancers without methylation ($P=0.04$) (Figure 3c). Considering that surgical cancer specimens are contaminated with normal cells, the findings here supported that *FHL1* was methylation-silenced also in surgical cancer specimens.

Association between *FHL1* methylation and the CpG island methylator phenotype

Clinicopathological characteristics of cancers with *FHL1* methylation were analyzed in the 80 gastric cancers. *FHL1* methylation was not associated with tumor invasion, lymph node metastasis and histological type (Table 1). In contrast, *FHL1* methylation was associated with the presence of the CGI methylator phenotype (CIMP), 17 of 21 cancers with *FHL1* methylation (81%) and 13 of 59 without being CIMP-positive (22%; $P=2.9\times10^{-6}$). *FHL1* methylation was associated with the presence of Epstein–Barr virus (EBV) infection ($P=0.02$), but not with *hMLH1* methylation. This suggested that, between the two subtypes of CIMP-positive gastric cancers (those with EBV infection and those with *hMLH1* methylation),[29] *FLH1* methylation was associated with the former.

Growth-suppressive activity of *FHL1*

The effect of the *FHL1* expression loss on cell growth was analyzed by knocking down *FHL1* first *in vitro*. Two *FHL1*-specific shRNAs (sh1and sh2), along with a control shRNA (luciferase-specific shRNA; Luc-sh), were introduced into two cancer cell lines with *FHL1* expression (HCT116 and HSC39). *FHL1* expression was confirmed to be strongly suppressed by sh1 (11.7% of the control cells) and sh2 (14.8%) by qRT–PCR and also by western blot (Figure 4a). *FHL1* knockdown accelerated cell growth in HCT116 cells (sh1, 243% of control cells at 120 h, $P<0.001$, and sh2, 191%, $P<0.001$) and in HSC39 cells (sh1, 144% of control cells at 96 h, $P<0.01$, and sh2, 130%, $P<0.01$) (Supplementary Figure 1). Then, *in vivo* growth assay using a nude mouse xenograft model showed that HCT116 cells with *FHL1* knockdown formed 2.7-fold larger tumors than control cells (Luc-sh) ($P<0.001$) (Figure 4b), and that their mean weight was 2.8-fold heavier than that of control cells (Figure 4c). The maintenance of *FHL1* decrease by shRNA was confirmed (Supplementary Figure 2).

The growth-suppressive activity was further analyzed by expressing exogenous *FHL1* in two non-expressing cell lines (AGS and MKN28). By qRT–PCR and western blot, expression levels of the exogenous *FHL1* in AGS and MKN28 were shown to be ~10-and 40-fold, respectively, of those in non-cancerous gastric mucosae (Figures 4d and 5a, and Supplementary Figure 3a). *FHL1* expression reduced the cell growth in AGS (72.2% of control

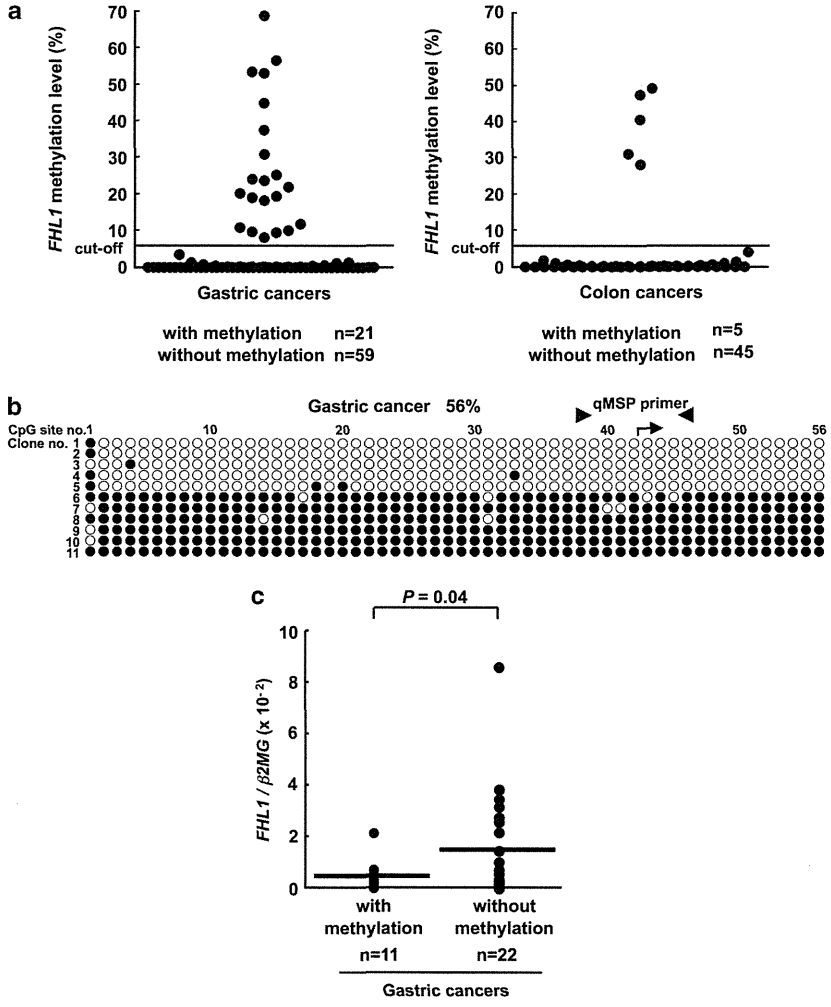

Figure 3. Methylation of *FHL1* in surgical gastrointestinal cancer specimens and its effect on expression. (**a**) Methylation levels in gastric (left) and colon (right) cancers derived from male patients. A horizontal line shows a cutoff value of 6%. *FHL1* was methylated in 21 of 80 primary gastric cancers and 5 of 50 colon cancers, respectively. (**b**) Confirmation of *FHL1* methylation by bisulfite sequencing. Fifty-six CpG sites were analyzed in a gastric cancer with a methylation level of 56%, and six of 11 DNA molecules were densely methylated. Closed circle, methylated CpG site; open circle, unmethylated CpG site; arrowheads, primers for qMSP; and arrow, transcription start site. (**c**) Decreased expression of *FHL1* in gastric cancers with methylation analyzed by qRT–PCR. A horizontal line represents the mean expression level in each group.

cells at 120 h, $P<0.05$; Figures 4d and 5b) but not in MKN28 (Supplementary Figure 3b).

Inhibitory effects of *FHL1* on migration and invasion

To clarify the mechanisms of how *FHL1* works as a tumor-suppressor gene, inhibitory effects of *FHL1* on cell migration and invasion were analyzed in two cell lines (AGS and MKN28). *FHL1* inhibited cell migration both in AGS (26.6% of control cells, $P<0.01$, Figure 5c) and in MKN28 (33.1% of control cells, $P<0.01$, Supplementary Figure 3c). In addition, *FHL1* inhibited cell invasion both in AGS ($P<0.05$, Figure 5d) and in MKN28 ($P<0.05$, Supplementary Figure 3d). In contrast, no induction of apoptosis was observed in AGS by terminal deoxynucleotidyl transferase dUTP nick end labeling assay (Supplementary Figure 4).

An *FHL1* mutation and its loss of function

FHL1 mutations were analyzed by sequencing its seven exons in 58 gastric and 144 colon cancer specimens derived from male patients. A somatic mutation (G642T; Lys214Asn) in exon 6 was identified in a colon cancer (Figure 5e). Also, a synonymous polymorphism (C450T) was observed in two gastric cancers. In the cancer with the G642T mutation, *FHL1* methylation was absent (data not shown), suggesting that either this mutation or promoter methylation was sufficient to inactivate *FHL1*. Further, the effects of the G642T mutation were analyzed by exogenously expressing the mutant and wild-type *FHL1* at similar levels (Figure 5a and Supplementary Figure 3a) in non-expressing AGS and MKN28 cells. The mutant *FHL1* lacked the inhibitory effects on migration and invasion both in AGS (Figures 5c and d) and in MKN28 (Supplementary Figures 3c and d). The mutant *FHL1* also lacked its inhibitory effect on cell growth in AGS (Figure 5b), whereas such effect could not be analyzed in MKN28, whose growth was not suppressed even by wild-type *FHL1*. These data indicated that the mutation was a loss-of-function mutation.

FHL1 methylation levels in non-cancerous gastric and colonic mucosae

To analyze the association between *FHL1* methylation and *Helicobacter pylori* (*H. pylori*) infection, and the contribution of

Table 1. Association between clinicopathological characteristics of patients and *FHL1* promoter methylation

Characteristics	*FLH1 methylation*		P
	Positive (N = *21*)	*Negative* (N = *59*)	
Tumor invasion			
⩽T2	13	33	0.80
>T2	8	26	
Lymph node metastasis			
Positive	15	50	0.20
Negative	6	9	
Histological type			
Intestinal	8	27	0.61
Diffuse	13	32	
CIMP			
Positive	17	13	2.9×10^{-6}
Negative	4	46	
EBV infection			
Positive	4	1	0.02
Negative	17	58	
hMLH1 *methylation*			
Positive	4	5	0.23
Negative	17	54	

Abbreviations: CIMP, CGI methylator phenotype; EBV, Epstein–Barr virus.

FHL1 methylation to the formation of an epigenetic field defect, *FHL1* methylation levels were quantified in gastric mucosae of male healthy volunteers (with and without *H. pylori* infection; 16 each) and non-cancerous mucosae of male gastric cancer patients (with and without *H. pylori* infection; 26 each) (Figure 6a). Among the healthy volunteers, *FHL1* methylation was elevated only in *H. pylori*-positive individuals (10 of 16, 62.5%; $P = 0.01$, *t*-test). As potent methylation induction by *H. pylori* can mask a difference in *H. pylori*-positive individuals,[8] *FHL1* methylation levels were compared between healthy volunteers and gastric cancer patients among the *H. pylori*-negative individuals. *FHL1* methylation level was shown to be elevated only in gastric cancer patients (5 of 26, 19.2%; $P = 0.09$, *t*-test). In the case of the colon, *FHL1* methylation was elevated in colonic mucosae of only 2 of 50 colon cancer patients (4%) (Supplementary Figure 5).

FHL1 methylation levels in female specimens

FHL1 methylation levels were analyzed in female specimens, including gastric mucosae of healthy volunteers (18 with *H. pylori* infection and 10 without), those of gastric cancer patients (7 with *H. pylori* infection and 11 without) and one specimen of peripheral leukocytes (Figure 6b). As in male specimens, among the healthy volunteers, *FHL1* methylation levels were significantly elevated in *H. pylori*-positive individuals ($P = 0.01$, *t*-test). Among the *H. pylori*-negative individuals, they tended to be higher in cancer patients than those in healthy volunteers ($P = 0.06$, *t*-test). *FHL1* methylation levels in *H. pylori*-negative female specimens were expected to be 50% because *FHL1* is located on chromosome X, but its actual distribution was between 20 and 40%. Bisulfite sequencing of the *FHL1* promoter region showed that female specimens contained DNA molecules with sparse methylation of CpG sites (Figure 6c), which was in contrast with the dense methylation in cancer specimens (Figure 3b). It was considered that the inactive chromosome X had sparse methylation of the *FHL1* promoter region not detected by qMSP.

DISCUSSION

The *FHL1* gene on chromosome X was shown to be a tumor-suppressor gene in gastrointestinal cancers by the presence of its methylation-silencing, its inhibitory effects on migration, invasion and growth, and the presence of a loss-of-function mutation. Notably, a loss-of-function mutation was identified for the first time in any type of cancers. This added *FHL1* as a new member of 'risky' tumor-suppressor genes on chromosome X, and the first tumor-suppressor gene on chromosome X that can be inactivated by methylation-silencing. *FHL1* methylation was associated with *H. pylori* infection and strongly accumulated in gastric mucosae of gastric cancer patients. Together with the fact that *FHL1* is a tumor-suppressor gene, the accumulation of *FHL1* methylation was considered to contribute to the formation of a field for cancerization as a driver.

Downregulation of *FHL1* in surgical specimens has been reported in breast, renal, prostate,[23] gastric,[25] liver,[21] and lung cancers.[22] The downregulation was associated with short patient survival and deep invasion in gastric cancers,[25] and with poor differentiation in lung cancers.[22] As a mechanism for the downregulation, methylation silencing was described in bladder cancers.[24] Functionally, *FHL1* has been reported to suppress growth of lung, liver and breast cancer cells and transformed fibroblasts,[21,22,26,30] and migration and invasion of bladder cancer cells and transformed fibroblasts.[24,26] The data obtained here were in line with previous reports, and demonstrated that *FHL1* inhibits migration and invasion in gastrointestinal cancer cells.[22]

Mechanistically, FHL1 is characterized by the presence of four and a half highly conserved LIM domains, which are involved in a wide range of protein–protein interactions, including actin cytoskeleton, cellular signaling proteins and transcriptional machinery.[31] In hepatocellular carcinomas, FHL1 was shown to interact with Smad2 and activate TGF-β pathway independently of TGF-β.[21] In breast cancers, FHL1 was shown to interact with estrogen receptor-α and estrogen receptor-β, and repress estrogen-responsive gene transcription.[30] Proteins that interact with FHL1 in gastric and colonic epithelial cells have not been clarified yet. However, inactivation of the TGF-β pathway is known to be involved in these cancers,[32] and is a strong candidate mechanism of how *FHL1* inactivation is involved in these gastrointestinal cancers.

FHL1 methylation was present not only in cancer tissues, but also in non-cancerous gastric mucosae of gastric cancer patients (5 of 26) and in non-cancerous colonic mucosae of colon cancer patients (2 of 50). This showed, for the first time in any types of cancers, that *FHL1* methylation silencing is involved in the formation of the epigenetic field defect as a driver. So far, only a limited number of driver genes, including *CDKN2A*, *CDH1* and *LOX*, are known to be involved in the formation of an epigenetic field defect.[18] For those genes on autosomes, it is difficult to estimate what fraction of cells has biallelic methylation. In contrast, in the case of *FHL1*, its methylation level linearly correlates with the fraction of cells with its inactivation, and, even if its methylation level is low, the presence of its methylation is expected to bring a significant impact. *H. pylori* infection is known to induce aberrant methylation that consists of temporary and permanent components,[8,33] and the high methylation levels in individuals with current *H. pylori* infection were in accordance with this previous finding.

In females, approximately half of the DNA molecules were methylated, densely or sparsely, in gastric mucosae and peripheral leukocytes of healthy volunteers without *H. pylori* infection by bisulfite sequencing. As no methylated DNA molecules were detected in a male specimen, both the densely and sparsely methylated DNA molecules in female specimens were considered to be derived from the inactive X allele.[34] However, we were not able to demonstrate it because a polymorphism that can

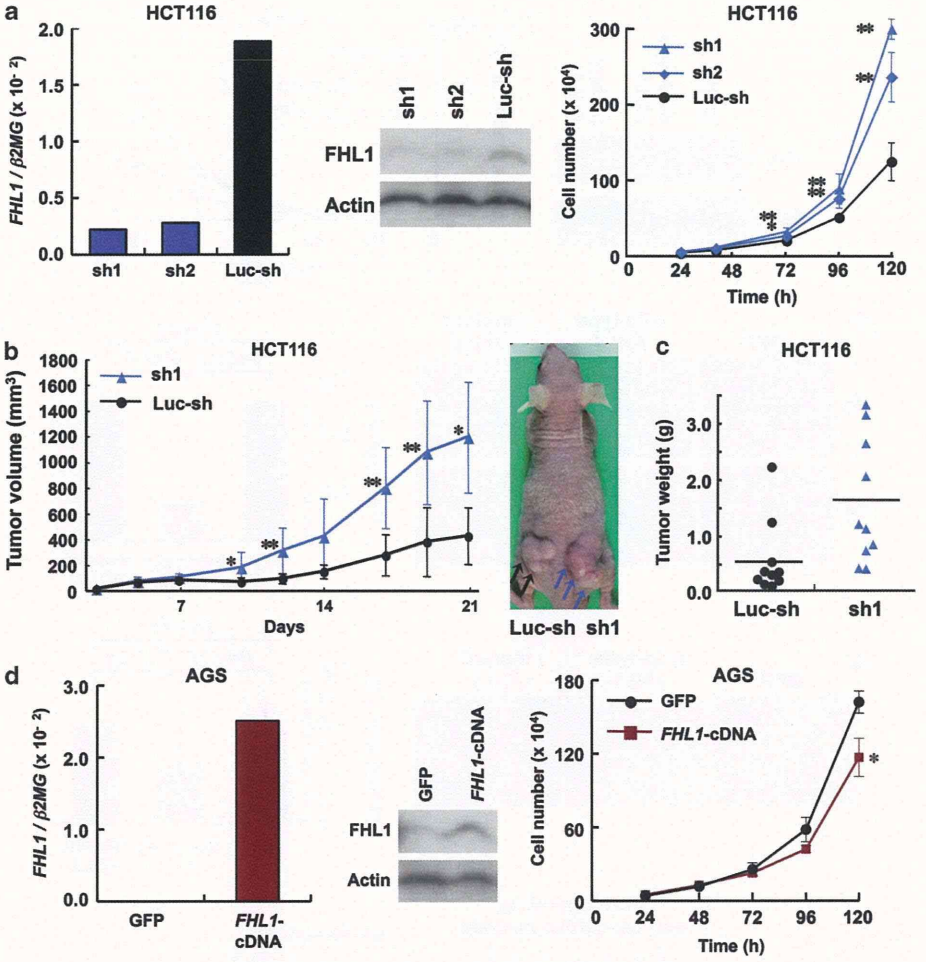

Figure 4. Growth-suppressive activity of *FHL1 in vitro* and *in vivo*. (**a**) *FHL1* knockdown and the resultant increased growth of HCT116 cells. Decreased expression of *FHL1* by its knockdown was confirmed by qRT–PCR (left) and western blot (middle). Growth rates of cells with *FHL1* knockdown were shown to be increased (*$P<0.01$, **$P<0.001$) (right). Data are shown as the mean of three independents ± s.d. (**b**) Increased *in vivo* growth of HCT116 cells with *FHL1* knockdown. Cells with *FHL1* knockdown (sh1) showed a 2.7-fold larger tumor volume compared with the control cells (Luc-sh) (*$P<0.01$, **$P<0.001$). Data are shown as the mean ± s.d. Arrows, tumors produced. (**c**) Increased tumor weight of cells with *FHL1* knockdown (sh1). Mean tumor weight of cells with knockdown (sh1) ($n=10$) was 2.8-fold heavier than that of controls (Luc-sh) ($n=10$). (**d**) Exogenous *FHL1* expression and the resultant decreased growth of AGS cells. Increased levels of *FHL1* expression were confirmed by qRT–PCR (left) and western blot (middle). Growth rates of cells with exogenous *FHL1* were shown to be significantly decreased (*$P<0.01$) (right).

distinguish the allelic origin of mRNA was not present. As qMSP detects only molecules that have dense methylation at primer sites, it was considered that it detected only densely methylated molecules, and methylation levels between 20 and 40% were observed in females.

In conclusion, we showed that *FHL1* on chromosome X is a methylation-silenced tumor-suppressor gene in gastrointestinal cancers, and its methylation in non-cancerous gastric mucosae contributes to the formation of an epigenetic field for cancerization.

MATERIALS AND METHODS

Cell lines and treatment with 5-aza-dC

Sixty-eight cancer cell lines (6 gastric, 7 colon, 12 lung, 12 skin, 7 pancreas, 4 esophageal, 4 prostate, 6 breast and 10 ovary cancer cell lines) and two normal colonic epithelial cells (CRL1790 and CRL1831) were obtained from the American Type Culture Collection (Manassas, VA, USA), Japanese Collection of Research Bioresources (Tokyo, Japan), RIKEN Cell Bank (Tsukuba, Japan) and Tohoku University Cell Resource Center for Biomedical Research (Sendai, Japan)(Supplementary Table 2). HSC39, HSC44 and HSC57 were gifted by Dr K Yanagihara; TMK1 was gifted by Dr W Yasui at Hiroshima University; and GC2 was established by MT For 5-aza-dC treatment. AGS and KATOIII cells were seeded on day 0; media containing freshly prepared 0.3 μM 5-aza-dC were added on days 1 and 3, and cells were harvested on day 5.[35]

Tissue specimens and analysis of *H. pylori* infection status

Cancer specimens were obtained from 80 male gastric cancer patients (average age = 60.4, range = 29–88) and 144 male colon cancer patients (average age = 70, range = 39–98) who underwent gastric and colon resection, respectively, with informed consent. All cancers were histologically diagnosed, and histological types of gastric cancers were classified according to the Lauren classification system (35 intestinal and 45 diffuse type).[36] EBV positivity was determined by *in situ* hybridization targeting *EBER1* using formalin-fixed and paraffin-embedded specimens.[37] The proportion of EBV-positive specimens (5 of 80, 6.3%) was close to EBV prevalence in a previous report (11 of 172, 6.4%).[38]

Normal-appearing gastric mucosae were obtained by endoscopic biopsy of the antral region from 60 healthy volunteers (32 male and 28 female; average age = 52, range = 25–91) and 70 gastric cancer patients

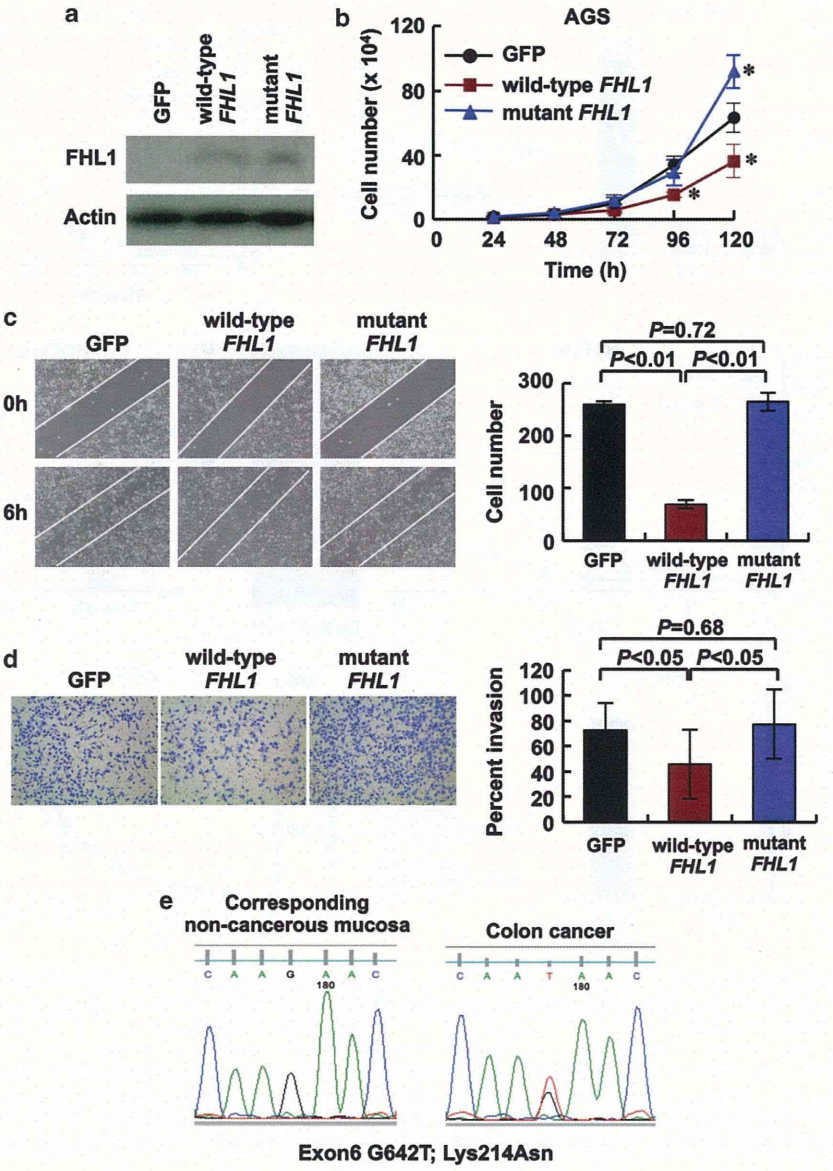

Figure 5. Inhibitory effects of *FHL1* on migration and invasion, and the lack of such functions in *FHL1* with the G642T mutation in AGS. (**a**) Expression levels of exogenous wild-type and mutant *FHL1* detected by western blot. (**b**) The growth-suppressive effect of the wild-type *FHL1*, and the lack of the effect in mutant *FHL1*. Whereas wild-type *FHL1* suppressed cell growth, mutant *FHL1* did not (*$P<0.01$). (**c**) Migration inhibition by wild-type *FHL1*, and the lack of the effect in the mutant *FHL1*. Whereas wild-type *FHL1* inhibited cell migration to 26.6% of the control cells, mutant *FHL1* did not. Photographs were taken at 0 and 6 h after scratching (left), and the number of cells that migrated into the scratched area was counted (mean ± s.d.; right). (**d**) Invasion inhibition by wild-type *FHL1*, and the lack of the effect in the mutant *FHL1*. Whereas wild-type *FHL1* inhibited cell invasion, mutant *FHL1* did not. Representative fields with invading cells on Matrigel-precoated membrane (left). Percent invasion is shown as the mean ± s.d. (right). (**e**) Sequence analysis of colon cancer specimens and corresponding non-cancerous colonic mucosae showed a somatic mutation (G642T; Lys214Asn) in exon 6 of *FHL1*.

(52 male and 18 female; average age = 65, range = 38–85). *H. pylori* infection status was analyzed by a serum anti-*H. pylori* IgG antibody test (SRL, Tokyo, Japan), rapid urease test (Otsuka, Tokushima, Japan) or culture test (Eiken, Tokyo, Japan). Gastric epithelial cells for qRT–PCR analysis were isolated by the gland isolation technique.[39] Normal-appearing colonic mucosae were obtained from a mucosal area distant from colon cancers of surgically resected specimens. Leukocytes were collected from one male (age = 47) and one female (age = 32) volunteer. Specimens were kept frozen at − 80 °C until DNA/RNA extraction. All the analyses using human-derived specimens were approved by the Institutional Review Boards.

Data processing of expression microarray analysis

Expression microarray analysis data in our previous report[19] were used. Signal intensities were scaled so that average signal intensity of all the 18 602 genes would become 500.

Sodium bisulfite modification, MSP, qMSP and bisulfite sequencing

Bisulfite modification was performed using 1 μg of *Bam*HI-digested genomic DNA as previously described.[40] MSP was performed with

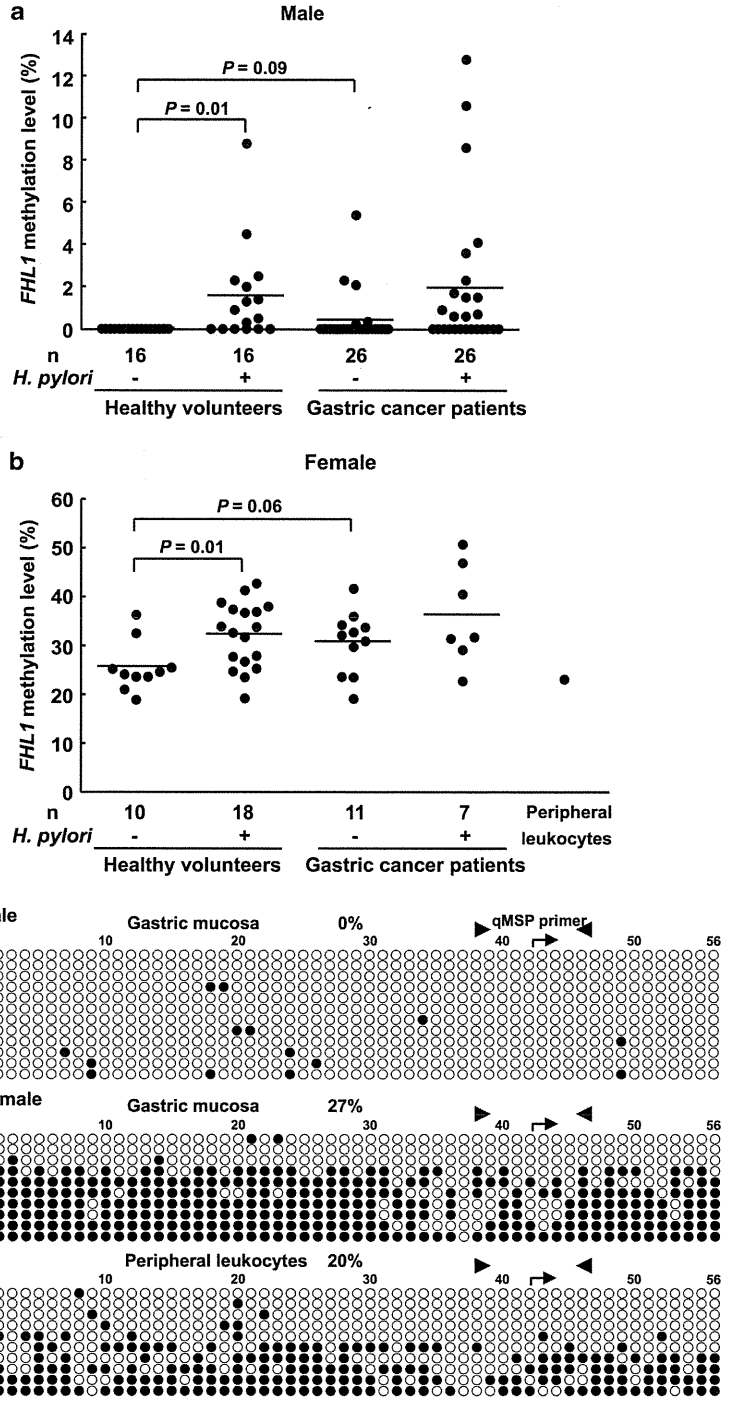

Figure 6. *FHL1* methylation levels in male and female gastric mucosae. (**a**) Methylation levels in male gastric mucosae of healthy volunteers and non-cancerous mucosae of gastric cancer patients. A horizontal line represents the mean methylation level for each group. Among healthy volunteers, *FHL1* methylation was present only in *H. pylori*-positive individuals ($P = 0.01$). Among individuals without *H. pylori* infection, *FHL1* methylation was present only in gastric cancer patients. (**b**) Methylation levels in female gastric mucosae and peripheral leukocytes. *FHL1* methylation levels distributed between 20 and 40%. Methylation levels were higher in *H. pylori*-positive healthy volunteers and gastric cancer patients also in female. (**c**) Bisulfite sequencing of male gastric mucosae, female gastric mucosae and female peripheral leukocytes. Female specimens contained both densely methylated and sparsely methylated DNA molecules, and it was considered that the inactive chromosome X can be densely and sparsely methylated. Closed circle, methylated CpG site; open circle, unmethylated CpG site; arrowheads, primers for qMSP; and arrow, transcription start site.

primer sets specific to methylated and unmethylated sequences (Supplementary Table 3). As controls, fully methylated and unmethylated DNA were prepared by methylating genomic DNA with *SssI* methylase (New England Biolabs, Beverly, MA, USA) and by amplifying genomic DNA with the GenomiPhi amplification system (GE Healthcare, Buckinghamshire, UK), respectively.

Quantitative real-time MSP was performed by real-time PCR using SYBR Green I (BioWhittaker Molecular Applications, Rockland, ME, USA) and an iCycler Thermal Cycler (Bio-Rad Laboratories, Hercules, CA, USA). Although a primer set for MSP was also used for qMSP, a specific annealing temperature in the presence of SYBR Green I was determined (Supplementary Table 3). The number of molecules in a specimen was determined by comparing its amplification with those of standard DNA that contained known numbers of molecules (10^1–10^6 molecules). Based on the numbers of methylated (M) and unmethylated (U) molecules, a methylation level was calculated as the fraction of M molecules in the total number of DNA molecules (no. of M molecules + no. of U molecules). Standard DNA was prepared by cloning PCR products of methylated and unmethylated sequences into a vector (pGEM-T Easy, Promega, Madison, WI, USA). The CIMP status in a gastric cancer was determined as described previously.[27]

Bisulfite sequencing was conducted with primers common to methylated and unmethylated DNA sequences (Supplementary Table 4). The PCR product was cloned into pGEM-T Easy, and 10–12 clones were cycle-sequenced for each specimen.

qRT–PCR

cDNA was synthesized from 1 μg of total RNA using a Superscript III (Invitrogen, Carlsbad, CA, USA). qRT–PCR was performed by real-time PCR using SYBR Green I and an iCycler Thermal Cycler. Standard DNA was prepared by serial dilution of PCR products quantified by the QIAxcel system (QIAGEN, Valencia, CA, USA) after purification using Zymo-Spin I Columns (Zymo Research, Orange, CA, USA).[41] The measured number of cDNA molecules was normalized to that of b2-microglobulin (*b2MG*). The primers and PCR conditions are shown in Supplementary Table 5.

Knockdown and cDNA introduction assays

For a knockdown assay, two pairs and one pair of oligonucleotides were designed against *FHL1* and *Luciferase* (control), respectively (Supplementary Table 6). After annealing of sense and antisense oligonucleotides, the fragment was cloned into a pGreenPuro lentiviral vector (System Biosciences, Mountain View, CA, USA). For cDNA cloning, the entire coding region of human *FHL1* was amplified by RT–PCR (Supplementary Table 7), and cloned into a pCDH-CMV-MCS-EF1-Puro lentiviral vector (System Biosciences). As a control, *copGFP* was cloned into the vector in the same manner. The mutant cDNA was synthesized using the site-directed mutagenesis technique.[42] Using complementary primers carrying mutated sequence (mutation site forward and reverse primers; Supplementary Table 7) and primers for each end of the entire coding region (entire region reverse and forward primers), RT–PCR was performed to generate two DNA fragments that had overlapping ends. These two PCR products were combined by a subsequent PCR with primers for each end of the entire coding region to obtain the mutant cDNA. The mutant cDNA was cloned into a pCDH-CMV-MCS-EF1-Puro lentiviral vector.

The viral vectors and packaging vectors (pPACKH1 HIV Lentivector Packaging Kit, System Biosciences) were cotransfected into 293TN packaging cells, and culture media-containing pseudoviral particles were retrieved. Infection of cancer cell lines with pseudoviral particles was performed according to the manufacturer's protocol (System Biosciences), and stably expressing cells were selected by puromycin without cloning.

Cell growth, migration, invasion and apoptosis analysis

Cell growth was analyzed by seeding cells in triplicate in a six-well plate (3×10^4 cells, AGS; 1×10^5 cells, HSC39) and in a 12-well plate (5×10^3 cells, HCT116). Their numbers were counted at 24, 48, 72, 96 and 120 h. Three independent cultures were performed for one experiment.

Cell migration was analyzed by a wound-healing assay.[43] Cells were seeded in triplicate in a 6-cm dish coated with type I collagen (1×10^6 cells, AGS; 4×10^6 cells, MKN28), and cultured in RPMI-1640 medium containing 1% fetal calf serum to form a monolayer. The cell monolayer was scraped in a straight line with a pipette tip. After incubation for 6 and 12 h, the migrating cells were observed under bright-field microscopy. Three independent cultures were performed for one experiment.

Cell invasion was analyzed by a Matrigel invasion assay, using a Boyden chamber with the Matrigel-precoated membrane or Matrigel-free membrane in the top chamber (BD Biosciences, Bedford, MA, USA). Cells were seeded in top chambers in serum-free RPMI1640 (5×10^4 cells, AGS; 1×10^5 cells, MKN28), and the bottom chambers were filled with RPMI1640 containing 10% fetal calf serum. After incubation for 24 and 48 h (AGS and MKN28, respectively), the area of cells invading through the top chambers was measured by ImageJ software (version 1.38, National Institutes of Health, Bethesda, MD, USA). Percent invasion was calculated as the area of cells invading through the Matrigel-precoated membrane relative to those through Matrigel-free membrane. Three independent cultures were performed for one experiment and the experiment was repeated three times.

The apoptosis of the cells was analyzed by terminal deoxynucleotidyl transferase dUTP nick end labeling assay, using an *in situ* cell death detection kit, TMRred (Roche, Basel, Switzerland).

Tumor formation assay in nude mice

Cells (8×10^6 cells, HCT116) were inoculated subcutaneously on both flanks of 7-week-old male athymic nude mice (BALB/cAJc1-nu/nu; CLEA, Tokyo, Japan). Tumor sizes were measured with calipers every 3 days and the volume was calculated as (length × width^2) × 0.5, and tumor weights were measured at their killing on day 22. All the animal experiments were approved by the Animal Experiment Ethical Committee at the National Cancer Center.

Mutation analysis

All seven exons of *FHL1* were amplified using 100 ng of genomic DNA with primers located in introns, except for one primer on exon 7 (Supplementary Table 8). The PCR products were directly cycle-sequenced with a BigDye Terminator kit (PE Biosystems, Foster City, CA, USA) and an ABI PRISM 310 automated DNA sequencer (PE Biosystems).

Statistical analysis

Differences in mean methylation levels, expression levels, cell numbers and tumor sizes were analyzed by the Welch *t*-test. Association between *FHL1* methylation and clinicopathological factors was analyzed by the χ^2 test. All the analyses were performed using SPSS (SPSS, Inc., Chicago, IL, USA), and the results were considered significant when a P value <0.05 was obtained by two-sided tests.

CONFLICT OF INTEREST

The authors declare no conflict of interest.

ACKNOWLEDGEMENTS

We thank Dr Yanagihara and Dr Yasui for their kind gift of cell lines. This study was supported by a Grant-in-Aid for the Third-term Comprehensive Cancer Control Strategy from the Ministry of Health, Labour and Welfare, Japan, and by the National Cancer Center Research and Development Fund. TA is a recipient of the Research Resident Fellowship from the Foundation for Promotion of Cancer Research.

REFERENCES

1 Knudson AG. Two genetic hits (more or less) to cancer. *Nat Rev Cancer* 2001; **1**: 157–162.
2 Ushijima T. Detection and interpretation of altered methylation patterns in cancer cells. *Nat Rev Cancer* 2005; **5**: 223–231.
3 Jones PA, Baylin SB. The epigenomics of cancer. *Cell* 2007; **128**: 683–692.
4 Rivera MN, Kim WJ, Wells J, Driscoll DR, Brannigan BW, Han M *et al.* An X chromosome gene, WTX, is commonly inactivated in Wilms tumor. *Science* 2007; **315**: 642–645.
5 Zuo T, Wang L, Morrison C, Chang X, Zhang H, Li W *et al.* FOXP3 is an X-linked breast cancer suppressor gene and an important repressor of the HER-2/ErbB2 oncogene. *Cell* 2007; **129**: 1275–1286.
6 Wang L, Liu R, Li W, Chen C, Katoh H, Chen GY *et al.* Somatic single hits inactivate the X-linked tumor suppressor FOXP3 in the prostate. *Cancer Cell* 2009; **16**: 336–346.
7 Van Vlierberghe P, Palomero T, Khiabanian H, Van Der Meulen J, Castillo M, Van Roy N *et al.* PHF6 mutations in T-cell acute lymphoblastic leukemia. *Nat Genet* 2010; **42**: 338–342.

8 Maekita T, Nakazawa K, Mihara M, Nakajima T, Yanaoka K, Iguchi M *et al.* High levels of aberrant DNA methylation in Helicobacter pylori-infected gastric mucosae and its possible association with gastric cancer risk. *Clin Cancer Res* 2006; **12**: 989–995.
9 Ando T, Yoshida T, Enomoto S, Asada K, Tatematsu M, Ichinose M *et al.* DNA methylation of microRNA genes in gastric mucosae of gastric cancer patients: its possible involvement in the formation of epigenetic field defect. *Int J Cancer* 2009; **124**: 2367–2374.
10 Shen L, Kondo Y, Rosner GL, Xiao L, Hernandez NS, Vilaythong J *et al.* MGMT promoter methylation and field defect in sporadic colorectal cancer. *J Natl Cancer Inst* 2005; **97**: 1330–1338.
11 Kondo Y, Kanai Y, Sakamoto M, Mizokami M, Ueda R, Hirohashi S. Genetic instability and aberrant DNA methylation in chronic hepatitis and cirrhosis—a comprehensive study of loss of heterozygosity and microsatellite instability at 39 loci and DNA hypermethylation on 8 CpG islands in microdissected specimens from patients with hepatocellular carcinoma. *Hepatology* 2000; **32**: 970–979.
12 Ishii T, Murakami J, Notohara K, Cullings HM, Sasamoto H, Kambara T *et al.* Oesophageal squamous cell carcinoma may develop within a background of accumulating DNA methylation in normal and dysplastic mucosa. *Gut* 2007; **56**: 13–19.
13 Oka D, Yamashita S, Tomioka T, Nakanishi Y, Kato H, Kaminishi M *et al.* The presence of aberrant DNA methylation in noncancerous esophageal mucosae in association with smoking history: a target for risk diagnosis and prevention of esophageal cancers. *Cancer* 2009; **115**: 3412–3426.
14 Lee YC, Wang HP, Wang CP, Ko JY, Lee JM, Chiu HM *et al.* Revisit of field cancerization in squamous cell carcinoma of upper aerodigestive tract: better risk assessment with epigenetic markers. *Cancer Prev Res* 2011; **4**: 1982–1992.
15 Yan PS, Venkataramu C, Ibrahim A, Liu JC, Shen RZ, Diaz NM *et al.* Mapping geographic zones of cancer risk with epigenetic biomarkers in normal breast tissue. *Clin Cancer Res* 2006; **12**: 6626–6636.
16 Arai E, Kanai Y, Ushijima S, Fujimoto H, Mukai K, Hirohashi S. Regional DNA hypermethylation and DNA methyltransferase (DNMT) 1 protein overexpression in both renal tumors and corresponding nontumorous renal tissues. *Int J Cancer* 2006; **119**: 288–296.
17 Nakajima T, Maekita T, Oda I, Gotoda T, Yamamoto S, Umemura S *et al.* Higher methylation levels in gastric mucosae significantly correlate with higher risk of gastric cancers. *Cancer Epidemiol Biomarkers Prev* 2006; **15**: 2317–2321.
18 Ushijima T. Epigenetic field for cancerization. *J Biochem Mol Biol* 2007; **40**: 142–150.
19 Yamashita S, Tsujino Y, Moriguchi K, Tatematsu M, Ushijima T. Chemical genomic screening for methylation-silenced genes in gastric cancer cell lines using 5-aza-2′-deoxycytidine treatment and oligonucleotide microarray. *Cancer Sci* 2006; **97**: 64–71.
20 Ushijima T, Watanabe N, Shimizu K, Miyamoto K, Sugimura T, Kaneda A. Decreased fidelity in replicating CpG methylation patterns in cancer cells. *Cancer Res* 2005; **65**: 11–17.
21 Ding L, Wang Z, Yan J, Yang X, Liu A, Qiu W *et al.* Human four-and-a-half LIM family members suppress tumor cell growth through a TGF-beta-like signaling pathway. *J Clin Invest* 2009; **119**: 349–361.
22 Niu C, Liang C, Guo J, Cheng L, Zhang H, Qin X *et al.* Downregulation and growth inhibitory role of FHL1 in lung cancer. *Int J Cancer* 2012; **130**: 2549–2556.
23 Li X, Jia Z, Shen Y, Ichikawa H, Jarvik J, Nagele RG *et al.* Coordinate suppression of Sdpr and Fhl1 expression in tumors of the breast, kidney, and prostate. *Cancer Sci* 2008; **99**: 1326–1333.
24 Matsumoto M, Kawakami K, Enokida H, Toki K, Matsuda R, Chiyomaru T *et al.* CpG hypermethylation of human four-and-a-half LIM domains 1 contributes to migration and invasion activity of human bladder cancer. *Int J Mol Med* 2010; **26**: 241–247.
25 Sakashita K, Mimori K, Tanaka F, Kamohara Y, Inoue H, Sawada T *et al.* Clinical significance of loss of Fhl1 expression in human gastric cancer. *Ann Surg Oncol* 2008; **15**: 2293–2300.
26 Shen Y, Jia Z, Nagele RG, Ichikawa H, Goldberg GS. SRC uses Cas to suppress Fhl1 in order to promote nonanchored growth and migration of tumor cells. *Cancer Res* 2006; **66**: 1543–1552.
27 Enomoto S, Maekita T, Tsukamoto T, Nakajima T, Nakazawa K, Tatematsu M *et al.* Lack of association between CpG island methylator phenotype in human gastric cancers and methylation in their background non-cancerous gastric mucosae. *Cancer Sci* 2007; **98**: 1853–1861.
28 Ota N, Kawakami K, Okuda T, Takehara A, Hiranuma C, Oyama K *et al.* Prognostic significance of p16(INK4a) hypermethylation in non-small cell lung cancer is evident by quantitative DNA methylation analysis. *Anticancer Res* 2006; **26**: 3729–3732.
29 Matsusaka K, Kaneda A, Nagae G, Ushiku T, Kikuchi Y, Hino R *et al.* Classification of Epstein-Barr virus-positive gastric cancers by definition of DNA methylation epigenotypes. *Cancer Res* 2011; **71**: 7187–7197.
30 Ding L, Niu C, Zheng Y, Xiong Z, Liu Y, Lin J *et al.* FHL1 interacts with oestrogen receptors and regulates breast cancer cell growth. *J Cell Mol Med* 2011; **15**: 72–85.
31 Shathasivam T, Kislinger T, Gramolini AO. Genes proteins and complexes: the multifaceted nature of FHL family proteins in diverse tissues. *J Cell Mol Med* 2010; **14**: 2702–2720.
32 Achyut BR, Yang L. Transforming growth factor-beta in the gastrointestinal and hepatic tumor microenvironment. *Gastroenterol* 2011; **141**: 1167–1178.
33 Niwa T, Tsukamoto T, Toyoda T, Mori A, Tanaka H, Maekita T *et al.* Inflammatory Processes Triggered by Helicobacter pylori Infection Cause Aberrant DNA Methylation in Gastric Epithelial Cells. *Cancer Res* 2010; **70**: 1430–1440.
34 Panning B, Jaenisch R. RNA and the epigenetic regulation of X chromosome inactivation. *Cell* 1998; **93**: 305–308.
35 Moriguchi K, Yamashita S, Tsujino Y, Tatematsu M, Ushijima T. Larger numbers of silenced genes in cancer cell lines with increased de novo methylation of scattered CpG sites. *Cancer Lett* 2007; **249**: 178–187.
36 Lauren P. The two histological main types of gastric carcinoma: diffuse and so-called intestinal-type carcinoma. An attempt at a histo-clinical classification. *Acta Pathol Microbiol Scand* 1965; **64**: 31–49.
37 Fukayama M, Hayashi Y, Iwasaki Y, Chong J, Ooba T, Takizawa T *et al.* Epstein-Barr virus-associated gastric carcinoma and Epstein-Barr virus infection of the stomach. *Lab Invest* 1994; **71**: 73–81.
38 Luo B, Wang Y, Wang XF, Liang H, Yan LP, Huang BH *et al.* Expression of Epstein-Barr virus genes in EBV-associated gastric carcinomas. *World J Gastroenterol* 2005; **11**: 629–633.
39 Cheng H, Bjerknes M, Amar J. Methods for the determination of epithelial cell kinetic parameters of human colonic epithelium isolated from surgical and biopsy specimens. *Gastroenterol* 1984; **86**: 78–85.
40 Kaneda A, Kaminishi M, Sugimura T, Ushijima T. Decreased expression of the seven ARP2/3 complex genes in human gastric cancers. *Cancer Lett* 2004; **212**: 203–210.
41 Hosoya K, Yamashita S, Ando T, Nakajima T, Itoh F, Ushijima T. Adenomatous polyposis coli 1A is likely to be methylated as a passenger in human gastric carcinogenesis. *Cancer Lett* 2009; **285**: 182–189.
42 Ho SN, Hunt HD, Horton RM, Pullen JK, Pease LR. Site-directed mutagenesis by overlap extension using the polymerase chain reaction. *Gene* 1989; **77**: 51–59.
43 Liang CC, Park AY, Guan JL. *In vitro* scratch assay: a convenient and inexpensive method for analysis of cell migration *in vitro*. *Nat Protoc* 2007; **2**: 329–333.

Supplementary Information accompanies the paper on the Oncogene website (http://www.nature.com/onc)

RESEARCH ARTICLE

Inflammation Enhanced X-irradiation-Induced Colonic Tumorigenesis in the Min mouse

Ayumi Nojiri[1,2], Takeshi Toyoda[1,3], Takuji Tanaka[4], Toshimichi Yoshida[2], Masae Tatematsu[1], Tetsuya Tsukamoto[1,2,5]*

Abstract

Inflammation is potential risk factor of various human malignancies. Inflammatory bowel syndromes such as ulcerative colitis are well known as risk factors for colon cancer. Here, we examined enhancing effects of dextran sulfate sodium (DSS)-associated inflammation on X-irradiation induced colonic tumorigenesis in Min and wild-type (WT) mice. Animals were X-irradiated at 1.5 Gy at 5 weeks of age (at 0 experimental week) and 2% DSS in drinking water was administered at 5 or 11 experimental weeks. Mice were sacrificed at 16 weeks and incidence and multiplicity of colonic tumors were assessed. Incidence of colonic tumors in Min mouse was increased from 33.3% to 100% ($p<0.05$) with X-irradiation alone, whereas no tumors were developed in WT mice. In DSS-treated Min mice, X-irradiation increased the number of colonic tumors. Total number of colonic tumors was increased 1.57 times to 30.7±3.83 tumors/mouse with X-irradiation+DSS at 5 weeks comapared to 19.6±2.9 in corresponding DSS alone group ($p<0.05$). When the duration of inflammation was compared, longer period of DSS effect promoted more colonic tumorigenesis. Collectively, we conclude that X-irradiation and DSS-induced inflammation act synergistically for colonic tumorigenesis.

Keywords: Min mouse - X-irradiation - DSS - colon

Asian Pac J Cancer Prev, **14 (7)**, 4135-4139

Introduction

Inflammation has been widely known as strong risk and promoting factor of carcinogenesis (Balkwill and Mantovani, 2001) in various types of human cancers (Ohshima et al., 2003). Among them, ulcerative colitis is in high risk condition in colonic carcinogensis (Munkholm, 2003). In the animal counterpart, dextran sulfate sodium (DSS) (Okayasu et al., 1990) showed powerful tumor promoting effect in murine colonic carcinogenesis models initiated with azoxymethane (AOM) (Tanaka et al., 2003), 1,2-dimethylhydrazine (DMH) (Kohno et al., 2005), and 2-amino-1-methyl-6-phenylimidazo[4,5-b]pyridine (PhIP) (Tanaka et al., 2005).

Familial adenomatous polyposis (FAP) is an inherited human disease characterized by numerous colorectal tumorigenesis (Kinzler and Vogelstein, 1996). FAP is caused by mutation in the adenomatous polyposis coli (APC) tumor suppressor gene (Powell et al., 1993). Min (multiple intestinal neoplasia) mouse is a murine model of human FAP (Moser et al., 1990), which has nonsense mutation at codon 850 in Apc gene (Su et al., 1992). The mouse develops multiple intestinal adenomas with inactivation of wild type allele. Min mouse have been revealed to be highly susceptible to carcinogenic agents. Subcarcinogenic low-dose *N*-ethyl-*N*-nitrosourea (ENU) increased the tumor incidence in the intestine and mammary gland in Min mice (Shoemaker et al., 1995). Other colonic carcinogens including PhIP (Steffensen et al., 1997) and AOM (Paulsen et al., 2003) also increased intestinal tumors. Besides chemical carcinogens, Min mice have been revealed to be susceptible to ionizing radiation (Luongo and Dove, 1996) in the age-dependent manner (Okamoto and Yonekawa, 2005). Inflammatory stimuli by DSS strongly induced colonic neoplasia in Min mice (Tanaka et al., 2006).

In this study, we investigated whether DSS-induced inflammation enhanced colorectal tumorigenesis initiated with low-dose X-irradiation in Min mice.

Materials and Methods

Animals and genotyping

Male C57BL/6J-ApcMin/J (Min) mice were purchased from The Jackson Laboratory (Bar Harbor, Maine, USA). Female wild type (WT) C57BL6/J were obtained from Clea Japan (Tokyo, Japan). They were housed in plastic cages with hardwood chips in an air-conditioned room

*[1]Division of Oncological Pathology, Aichi Cancer Center Research Institute, Nagoya, [2]Department of Pathology and Matrix Biology, Mie University Graduate School of Medicine, Tsu, [3]Division of Pathology, National Institute of Health Sciences, Tokyo, [4]The Tohkai Cytopathology Institute, Cancer Research and Prevention, Gifu, [5]Department of Diagnostic Pathology, Fujita Health University School of Medicine, Toyoake, Japan *For correspondence: ttsukamt@fujita-hu.ac.jp*

with 12 h light-12 h dark cycle and were given basal diet (OA-2, Clea Japan) and water *ad libitum*. One male Min mouse and 5 female wild type C57BL6/J were mated and offsprings were subjected to genotyping. DNA samples were extracted from their tails using a QIAamp tissue kit (QIAGEN, Tokyo, Japan). The 10 μl PCR reaction mixture consited of TITANIUM Taq DNA polymerase (Clontech, Mountain View, CA, USA), 1x buffer provided, 1x dNTP, 1μM of PCR primers (named oIMR0033, oIMR0034, and oIMR0758) and 1μl of genomic DNA. oIMR0033 (5'- GCC ATC CCT TCA CGT TAG -3') and oIMR0034 (5'- TTC CAC TTT GGC ATA AGG C -3') are forward and reverse wild type primers, respectively, to amplify common region. oIMR0758 is forward Min specific primer (5'- TTC TGA GAA AGA CAG AAG TTA -3') in which final adenosin residue corresponds to the mutation. PCR was performed using a Veriti thermal cycler (Applied Biosystems, Life Technologies, Carlsbad, CA, USA) as follows: 1 cycle of 95°C for 1 min; 35 cycles of 95°C for 30 sec, 65°C for 30 sec, 68°C for 30 sec; 1 cycle of 68°C for 3 min. The reaction mixture was electrophoresed in 0.8% SeaKem GTG agarose gel (Cambrex, East Rutherford, NJ, USA). Animals were judged as Min, if 340 bp band was appeared; both of wild type and Min genotypes possessed 600 bp band encompassing the mutation residue.

Experimental design

The experimental design is shown in Figure 1. Min mice and littermate WT mice were randomly divided into 6 groups (groups A–D). Single whole-body irradiation was given to five week-old animals at 1.5 Gy using an X-ray irradiator (MBR-1520R-3, Hitachi Power Solutions Co., Ltd., Tokyo, Japan) with a 0.5 mm Al+0.2 mm Cu filter in Groups C, D, and F. Dose of X-irradiation was determined to be lower than the previous report (Okamoto and Yonekawa, 2005) to compare enhancing effect of dextran sulfate sodium (DSS). DSS with a molecular weight of 40,000 was purchased from ICN Biochemicals, Inc. (Aurora, OH, USA), dissolved in water at a concentration of 2% (w/v), and administered at 5 experimental week in Groups E and F or at 11 week in Groups B and D for 1 week. The animals were sacrificed at 16 week. Total colon and cecum were fixed in 10% neutral buffered formalin or methacarn and stained with 0.2% methylene blue. Colon segments (S) were divided from S1 to S4 and cecum as S5 (Figure 2). The number of colonic tumors was counted in each segment. The experimental design was approved by the Animal Care Committee of the Aichi Cancer Center Research Institute, and the animals were cared for in accordance with institutional guidelines as well as the Guidelines for Proper Conduct of Animal Experiments (Science Council of Japan, June 1, 2006).

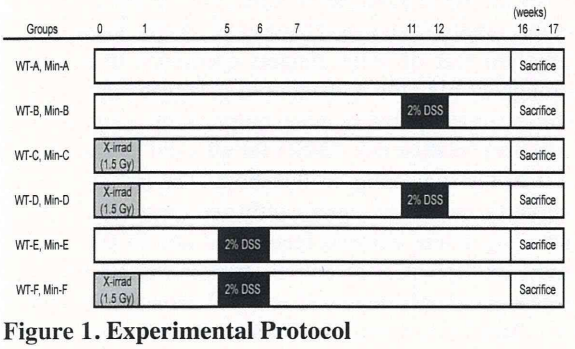

Figure 1. Experimental Protocol

Statistical analysis

The significance of difference in the incidence of colonic tumors was calculated using Fischer's exact test. Tumor multiplicities were analyzed with Mann-Whitney *U* test. Differences were considered as statistically significant if $p<0.05$.

Results

Incidence of colon tumors in WT and Min mice

Effective numbers of animals are described in Table 1. In the wild type mice, incidence of Group WT-D (33.3%) is significantly higher than that of Group WT-C (0%), suggesting enhancing results of DSS on X-irradiated tumorigenesis ($p<0.05$).

When Groups Min-A and Min-C were compared in Min mice, incidence of Group C (100%) was higher than that of Group A (33.3%), proving the aggravating effect of X-irradiation especially in Min mice ($p<0.002$).

When the two genotypes were compared in each group, Min mice showed increased incidence with statistical significance in Groups B-F (Table 1).

Multiplicity of colon tumors in Min mice

X-irradiation at 1.5 Gy alone [the number of tumors=0.91±0.21 (Ave±SE)/mouse in Group C] increased the number of colon tumors in S2 compared with the corresponding region in Group A (0.25±0.13/mouse, $p<0.05$). Total number was also augmented (2.55±0.41 and 1.33±0.45/mouse in Groups C and A, respectively,

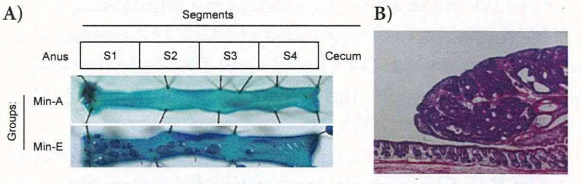

Figure 2. Macroscopic View and Histology of Colon Tumor. A) Macroscopic view of colonic mucosa. Total colon is divided to S1-S4. Cecum is S5 (not shown). Methylene blue staining. **B)** Representative histology of colonic tumor. Hematoxylin and eosin staining. Original magnification, 50x

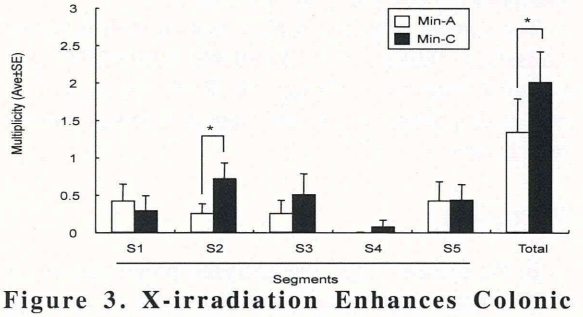

Figure 3. X-irradiation Enhances Colonic Tumorigenesis in Min mice without DSS. Group Min-A (Open bar) and Min-C (Closed bar). *$p<0.05$